HHS Public Access

Author manuscript

Knowl Based Syst. Author manuscript; available in PMC 2018 August 15.

Published in final edited form as:

Knowl Based Syst. 2017 August 15; 130: 33–50. doi:10.1016/j.knosys.2017.05.018.

Knowledge-leveraged transfer fuzzy *C*-Means for texture image segmentation with self-adaptive cluster prototype matching

Pengjiang Qian[a,b,c], **Kaifa Zhao**[a], **Yizhang Jiang**[a,*], **Kuan-Hao Su**[b,c], **Zhaohong Deng**[a], **Shitong Wang**[a], and **Raymond F. Muzic Jr.**[b,c]

[a]School of Digital Media, Jiangnan University, Wuxi, Jiangsu, PR China

[b]Case Center for Imaging Research, Case Western Reserve University, Cleveland, Ohio, USA

[c]Department of Radiology, University Hospitals Cleveland Medical Center, Case Western Reserve University, Cleveland, Ohio, USA

Abstract

We study a novel fuzzy clustering method to improve the segmentation performance on the target texture image by leveraging the knowledge from a prior texture image. Two knowledge transfer mechanisms, i.e. *knowledge-leveraged prototype transfer* (KL-PT) and *knowledge-leveraged prototype matching* (KL-PM) are first introduced as the bases. Applying them, the *knowledge-leveraged transfer fuzzy C-means* (KL-TFCM) method and its three-stage-interlinked framework, including knowledge extraction, knowledge matching, and knowledge utilization, are developed. There are two specific versions: KL-TFCM-c and KL-TFCM-f, i.e. the so-called crisp and flexible forms, which use the strategies of maximum matching degree and weighted sum, respectively. The significance of our work is fourfold: 1) Owing to the adjustability of referable degree between the source and target domains, KL-PT is capable of appropriately learning the insightful knowledge, i.e. the cluster prototypes, from the source domain; 2) KL-PM is able to self-adaptively determine the reasonable pairwise relationships of cluster prototypes between the source and target domains, even if the numbers of clusters differ in the two domains; 3) The joint action of KL-PM and KL-PT can effectively resolve the data inconsistency and heterogeneity between the source and target domains, e.g. the data distribution diversity and cluster number difference. Thus, using the three-stage-based knowledge transfer, the beneficial knowledge from the source domain can be extensively, self-adaptively leveraged in the target domain. As evidence of this, both KL-TFCM-c and KL-TFCM-f surpass many existing clustering methods in texture image segmentation; and 4) In the case of different cluster numbers between the source and target domains, KL-TFCM-f proves higher clustering effectiveness and segmentation performance than does KL-TFCM-c.

Keywords

Fuzzy C-means (FCM); Transfer learning; Knowledge transfer; Image segmentation; Data heterogeneity

*Corresponding author: qianpjiang@jiangnan.edu.cn (P. Qian), jyz0512@163.com (Y. Jiang).

1. Introduction

The effectiveness of clustering methods is often largely influenced by noise existing in target data sets. Usually, the greater the noise amplitude, the more negative the impact is. However, noise is nearly unavoidable and particularly impacts image segmentation [1–5], which motivates our research. Specifically, we address the issue that the segmentation performance of classic fuzzy *C*-means (FCM) [6–8], one of the most popular clustering approaches, is highly degraded by noise. While there have been numerous attempts to address this challenge, such as Ref. [1,2,9–15], most have not transcended the scope of traditional learning modalities and cannot achieve the required performance. In contrast, transfer learning [16,17], a state-of-the-art machine learning technique which will be introduced in the next section, has triggered an increasing amount of research interest owing to its distinctive advantages [18–42]. In brief, transfer learning helps one algorithm to improve the processing efficacy in the target domain, e.g. the image to be segmented, through the use of information in the source domain, e.g. another referenced image [16,22].

We pursue transfer learning as a means to improve the segmentation performance of FCM on target texture images in this manuscript. Specifically, the *knowledge-leveraged prototype transfer* (KL-PT) mechanism is introduced in response to the questions “What in the source domain can be enlisted as the knowledge?” and “How is such knowledge properly learned in the target domain?”. Further, to the challenge of performing knowledge transfer when the numbers of clusters in the source and target domains are inconsistent, the *knowledge-leveraged prototype matching* (KL-PM) mechanism is presented based on FCM. After that, via these two mechanisms, and with a three-stage-interlinked framework, i.e. knowledge extraction, knowledge matching, and knowledge utilization, the *knowledge-leveraged transfer fuzzy C-means* (KL-TFCM) approach is developed for the purpose of target texture image segmentation. In addition, by means of the strategies of maximum matching degree and weighted sum, KL-TFCM is differentiated into two specific versions: KL-TFCM-c and KL-TFCM-f, i.e. the crisp and flexible forms of the KL-TFCM, respectively. In summary, the contributions of our effort s are as follows:

1. KL-PT is devoted to leveraging the insightful knowledge, i.e., the cluster prototypes, of the source domain to guide the fuzzy clustering in the target domain, with the desirable adjustability of the referable degree between the source and target domains.
2. KL-PM strives to self-adaptively determine the pairwise relationships with regard to the cluster prototypes between the source and target domains, particularly when the numbers of clusters in the two domains are inconsistent.
3. By organically incorporating the strength of FCM, KL-PM, and KL-PT, and using the delicate three-stage-interlinked frame-work of knowledge transfer, we develop two versions of KL-TFCM methods, i.e., KL-TFCM-c and KL-TFCM-f, for the effective segmentation on target texture images. Both of them strive to properly leverage knowledge across domains, even though there is a certain extent of data inconsistency/heterogeneity between the source and target domains, e.g. the data distribution diversity and cluster number difference.

4. Benefiting from the more flexible strategy to generate cluster representatives from the source domain, compared with KL-TFCM-c, KL-TFCM-f exhibits better noise-tolerance as well as clustering effectiveness, particularly when the numbers of clusters differ in the source and target domains; this facilitates its generally preferable segmentation performance on target texture images.

Moreover, for knowledge-leveraged transfer clustering, our proposed KL-PT and KL-PM mechanisms are also suitable for other classic fuzzy clustering models, e.g., maximum entropy clustering (MEC) [43,44], fuzzy clustering by quadratic regularization (FC-QR) [43,45], and possibilistic C-means (PCM) [43,46] ; this additionally highlights our efforts in this manuscript.

The reminder in this manuscript is organized as follows. Section II reviews the theories and methods related to our research. Section III introduces, step-by-step, the knowledge transfer mechanisms regarding KL-PT and KL-PM, the KL-TFCM framework, and the two specific algorithms—KL-TFCM-c and KL-TFCM-f. Section IV evaluates the performance of KL-TFCM in texture image segmentation. Section V concludes and indicates areas of future work.

2. Related work

First, to facilitate understanding, common notations used throughout this paper are listed in Table 1.

2.1. Classic FCM

FCM attempts to group a set of given data instances, $X = \{\mathbf{x}_1,...\mathbf{x}_N\} \in R^{N\times D}$, into C disjoint clusters by means of the membership matrix $\mathbf{U} = [\mu_{ij}]_{C\times N}$ and the cluster prototypes $\mathbf{V} = [\mathbf{v}_1, \cdots, \mathbf{v}_C]^{\mathrm{T}}$. For this purpose, FCM adopts the following objective function:

$$\min \left(J_{\mathrm{FCM}}(\mathbf{U},\mathbf{V}) = \sum_{i=1}^{C}\sum_{j=1}^{N} \mu_{ij}^{m} \left\| \mathbf{x}_j - \mathbf{v}_i \right\|^2 \right) \quad (1)$$
$$\text{s.t. } \mu_{ij} \in [0,1] \text{ and } \sum_{i=1}^{C} \mu_{ij} = 1, \ j \in [1,N]$$

where $m > 1$ is the fuzzifier, i.e. the weighting exponent that controls the fuzziness of partitions.

Via the Lagrange optimization, it is easy to derive the following updating rules for the cluster prototype $\mathbf{v}_i$ and membership degree μ_{ij}:

$$\mathbf{v}_i = \frac{\sum_{j=1}^{N} \mu_{ij}^m \mathbf{x}_j}{\sum_{j=1}^{N} \mu_{ij}^m} \quad (2)$$

$$\mu_{ij} = \frac{1}{\left[\sum_{k=1}^{C} \frac{\|\mathbf{x}_j - \mathbf{v}_i\|^2}{\|\mathbf{x}_j - \mathbf{v}_k\|^2}\right]^{\frac{1}{m-1}}} \quad (3)$$

Via the iterative procedure, the final fuzzy membership matrix **U** is attained, and then the cluster that each data instance should belong to can be determined in terms of the maximum probability principle.

As mentioned in Introduction, one disadvantage of FCM is its sensitivity to noise existing in target data sets which often incurs its inefficiency in target image segmentation.

2.2. Transfer learning based clustering and related methods

A. Transfer learning—Transfer learning [16–42] has recently become one of the hot topics in pattern recognition. Transfer learning focuses on improving the learning performance of intelligent algorithms on the target data set, i.e. the target domain, by referring to some beneficial information from the related data set, i.e. the source domain. Transfer learning is suitable for the situation where the target data are insufficient or distorted by noise or outliers, whereas some beneficial information from relevant data sets is available. Although the most common form of transfer learning entails only one source domain and one target domain, the number of source domains can be selected as needed.

The referable information between the source and target domains generally exhibits two types—*raw data* and *knowledge*. Due to the correlation between domains, some data in the source domain are certainly available supplements for those in the target domain. This is termed instance-transfer [16,33,34] in transfer learning. However, because of the difference of data distributions across domains, not all raw data in the source domain are beneficial to the target domain. To avoid the negative transfer [16,17,35], i.e. the phenomenon that source domain data or tasks contribute to the reduced performance of learning in the target domain, extracting knowledge instead of raw data from the source domain is a safe choose. In transfer learning, knowledge is referred to as a category of advanced information from the source domain, such as feature representations [16,17,25,36,37], parameters [16,21,39], and relationships [16,38], which is usually obtained from certain specific perspectives and via some reliable theories and precise procedures. Compared with raw data, knowledge is usually regarded as being more insightful as well as possessing stronger anti-noise capability. In some cases where the original data in the source domain are not accessible, for

instance, because of privacy protection, it could be the only feasible pathway for transfer learning to extract knowledge rather than raw data from the source domain.

In general, there have been three categories of transfer learning [16,17] so far, i.e. inductive transfer learning, transductive transfer learning, and unsupervised transfer learning. In inductive transfer learning, it is required to induce an objective predictive model based on the labeled data in the target domain and with the assistance of the data or knowledge from the source domain. Many transfer classification [17,18,21,39] and regression [26–28] methods belong to this category. Conversely, in transductive transfer learning, there is no labeled data in the target domain while lots of labeled data in the source domain are usually available. Some approaches of domain-adaptation-based transfer classification [40–42] are the representatives of this category. As for unsupervised transfer learning, such as the research of transfer clustering [31,32] and transfer dimensionality reduction [29,30], it is label-independent in both of the source and target domains. So far, existing work on unsupervised transfer learning is comparatively little, and this encourages our research in this manuscript. One can refer to [16,17] for the more complete surveys on transfer learning.

B. Transfer clustering—As is mentioned above, clustering specializes in grouping a set of data instances so that objects in the same group (namely, a cluster) are more similar to each other than to those in other groups (clusters). The practical effectiveness of clustering methods depends strongly on the data quantity and quality in the target data set. Conventional clustering techniques can achieve desirable clustering performance only in relatively ideal situations in which data are relatively sufficient and have little distortion by noise or outliers. Such conditions, however, are difficult to achieve in practice. Transfer learning based clustering has emerged as an approach to address this challenge [31,32,47].

We use a simple example having only one source domain along with the target domain, as shown in Fig. 1, to explain how clustering is associated with transfer learning. As is evident in Fig. 1 (b), noise interference causes the examples in the target data set (X_2) to be mixed together so that the three potential clusters, indicated by red, green, and black, are difficult to distinguish using conventional clustering methods. Suppose that another comparatively low-noise data set (X_1) is now available, as shown in Fig. 1 (a), in which the data essence can be relatively easily captured by usual clustering approaches. Regardless of the apparent distinction of cluster numbers in X_1 and X_2, there are intrinsic connections between these two data sets, e.g., the three potentially embedded clusters in X_2 also exist in X_1, although their individual data distributions are visually different, possibly due to noise. In such case, transfer learning is an appropriate strategy conducive to improving the clustering performance on X_2 by taking X_2 and X_1 as the target and source domains, respectively. If any fuzzy clustering method, e.g., FCM, is performed on X_1, the cluster prototypes (centroids) can be attained, as marked with small, blue stars in Fig. 1 (a). These achieved cluster prototypes in X_1 are reasonably regarded as a type of knowledge for guiding and improving the clustering accuracy on X_2. This is exactly the central idea of our knowledge-leveraged transfer clustering in this literature.

To date there have been few studies that connect transfer learning and clustering. The two well-known ones are the self-taught clustering (STC) [31] and transfer spectral clustering

(TSC) [32]. STC was a collaborative learning-based transfer clustering approach, which simultaneously clustered the target and auxiliary data with allowing the feature representation from the auxiliary data to influence the target data via the common features. Benefiting from the new data representation, STC worked well on the target data. As for TSC, it assumes that the embedded information regarding features could connect different clustering tasks of different data sets and hence mutually improve the clustering performance of both sets. As such, both the data manifold information of clustering tasks and the feature manifold information shared between related clustering tasks were involved in TSC. In addition, the collaborative clustering strategy was also recruited in TSC for controlling the knowledge transfer among tasks. Nevertheless, it should particularly be pointed out that, although STC and TSC have proved their respective advantages, both are restricted in the condition that the cluster numbers in the source and target domains are the same. That is, neither of them can be used for such transfer scenario wherein the number of clusters in one domain is different from that in the other. In addition, we have recently been attempting to establish the bridge between transfer learning and partition-based clustering [1,2,10]. For example, we introduced the concept of cluster prototype-based knowledge transfer [47] for many sof-tpartition clustering models, such as FCM, soft subspace clustering [10,48], and maximum entropy clustering [43,44]. Our research in this manuscript also belongs to this category.

C. Methods associated with transfer clustering—Despite the fact that transfer clustering only emerged in recent years, it is not isolated from other mainstream techniques in pattern recognition, such as multi-task clustering [49,50], co-clustering (collaborative clustering) [13,51,52], semi-supervised clustering [53,54,55], and supervised clustering [56,57,58].

Multi-task clustering concurrently performs clustering tasks with interactions among these tasks so that all of them achieve better performance versus clustering separately. For example, the *learning shared subspace for multitask clustering* (LSSMTC) [49] focused on learning a subspace shared by all the tasks, through which the knowledge of the tasks can be transferred to each other. Moreover, as the derivative of LSSMTC, the *multi-task clustering via domain adaptation* (MTC-DM) [50] was proposed in order to address the issue of distribution differences among tasks according to the frontier research in domain adaptation. As revealed in [16,17], transfer learning is actually one of the extensions of multi-task learning. The most noticeable difference between transfer clustering and multi-task clustering lies in that the former merely cares about the task occurred in the target domain whereas conventional multi-task clustering utilizes the data in all tasks directly. Thus, when multi-task clustering is used, a high noise level in one data set can cause negative consequences among tasks.

Co-clustering performs clustering on the data instances and attributes simultaneously on the target data set. Therefore, it is also capable of being regarded as a special type of multi-task clustering, in the sense of two collaborative clustering tasks from the perspectives of examples and features separately. In this aspect, considerable work has also been conducted. For instance, the *dual-regularized co-clustering* (DRCC) [51] was developed via semi-nonnegative matrix tri-factorization as well as manifold information. That is, by constructing

two graphs on the data points and features respectively, the co-clustering was formulated as semi-nonnegative matrix tri-factorization with two graph regularization terms, requiring that the cluster labels of data points are smooth to the data manifold, whereas those of features are smooth to the feature manifold. In addition, by treating the contingency table as an empirical joint probability distribution between two discrete random variables which take values over the rows and columns, the *information-theoretic co-clustering* (ITCC) [52] was put forward with maximizing mutual information between the clustered random variables subject to the constraints on the cluster numbers of row and column. As revealed in both STC [31] and TSC [32], co-clustering is sometimes involved in transfer clustering when feature-based knowledge is shared between the auxiliary and target data.

Semi-supervised clustering and supervised clustering are the other two categories of clustering techniques associated with transfer clustering. Both attempt to improve the clustering performance on target data sets via the assist of given prior information. This is consistent with the intention of transfer clustering. We briefly review them as follows.

Semi-supervised clustering aims to enhance the clustering performance using some side information, i.e. must-link and/or cannot-link constraints, on the target data set. The existing research on semi-supervised clustering can be subdivided into two major groups, i.e. similarity-based methods and search-based methods. The similarity-based method creates a modified distance function that incorporates the knowledge with respect to the given side information and use a conventional clustering model to cluster the data. For example, the *K*-means clustering in conjunction with one modified distance function was used to compute clusters in [54], and one shortest path algorithm [55] was developed by modifying the Euclidian distance function based on the prior knowledge of pairwise constraints. Conversely, the search-based method modifies the clustering algorithm itself but does not change the distance function. For instance, the *constrained K-means clustering* (CKM) [53] was developed by profitably manipulating the search procedure of classic *K*-means so as to make use of the pairwise must-link and cannot-link constraints.

Supervised clustering is to automatically adapt a clustering algorithm that learns a parameterized similarity measure with the aid of a training set consisting of numerous labeled examples. Differing from semi-supervised clustering, the learned parameterized similarity measure in supervised clustering is usually used to cluster future data sets rather than the current one for training. For instance, the *support vector machine-based supervised clustering approaches* [56,57] were studied by learning the item or item-pair based similarity measure to optimize the performance of correlation clustering on a variety of performance measures. In addition, a *supervised fuzzy C-means clustering method* (SFCM) [58] was presented by defining a multivariate Gaussian-based distance measure of which the parameters needs to be trained using the given labeled examples.

However, it should be pointed out that the applicable data scenes of semi-supervised clustering, supervised clustering, and transfer clustering are markedly different, regardless of the fact that the prior information, in the form of either raw data or advanced knowledge, is involved in all of them. Specifically, semi-supervised clustering usually serves only one data set. It gets some beneficial supervision information from one data set and eventually boosts

clustering on the same data set. In supervised clustering, a training set is given in which all examples are labeled. One parameterized distance measure, which aims to group future data sets, is then learned via these training data. Here the training set and future data sets are from the same domain in supervised clustering. As for transfer clustering, as already disclosed, the prior information is obtained from the source domain/domains but is used in the target domain, and there usually exist different degrees of data inconsistency between the source and target domains. Therefore, both semi-supervised clustering and supervised clustering can be regarded as the special cases of transfer learning in which the target and auxiliary data possess the same distribution.

3. Knowledge-leveraged transfer fuzzy C-Means (KL-TFCM) for texture image segmentation

Now coming back to the intent of this paper, we focus on exploring the promising fuzzy clustering schema for target texture image segmentation, based on transfer learning. Two points need to be clarified before introducing our work. First, only one source domain is considered throughout our current research. The multiple-source-domain-oriented model will be continued in the future. Second, we always suppose that the data in the source domain are relatively pure and sufficient so that we can achieve desirable, insightful knowledge to assist the clustering in the target domain.

Let us begin with one realistic scenario, as shown in Fig. 2, so as to intuitively illustrate how transfer clustering occurs in the texture image segmentation. Fig. 2 (c) is the target image to be segmented. It is distinctly intractable to deal with such image as it has been rather polluted by noise, and conventional clustering methods usually cannot gain insights into the essence, i.e. Fig. 2 (b). In such case, transfer learning can be adopted to obtain valuable information from another correlative texture image, i.e. Fig. 2 (a), in order to assist the eventual clustering on Fig. 2 (c). In the context of transfer learning, Fig. 2 (c) is the target domain and Fig. 2 (a) is the only source domain. What could be regarded as beneficial information (i.e. referable knowledge) across two domains are the intrinsic characteristics of common textures between Fig. 2 (a) and (b), similarly between Fig. 2 (a) and (c). Certainly, due to the noise distortion in Fig. 2 (c), the texture characteristics between Fig. 2 (a) and (c) are not distinctly consistent even if they are essentially the same textures, which actually depend on the referable degree between these two images (domains). Moreover, we also face two other challenges:

1. What can be recruited for effectively embodying the intrinsic texture characteristics in the referenced source image, so as to attain the desirable, valuable knowledge for transfer clustering on the target texture image?
2. How can one self-adaptively learn knowledge from the source domain, in answer to the probable data inconsistency (data heterogeneity) between the source and target domains, e.g., the data distribution diversity as well as the cluster number difference between Fig. 2 (a) and (c)?

For addressing the above issues, we detail our countermeasures as follows.

3.1. Self-adaptive, knowledge-leveraged transfer mechanisms across domains

As we know well, the resultant cluster centroids, $\mathbf{V} = [\mathbf{v}_1, \cdots, \mathbf{v}_C]^{\mathrm{T}}$, are also referred to as the cluster prototypes in fuzzy clustering, e.g. FCM, which means that each of them is able to represent the objects in its matching cluster [43]. Based on this, suppose under the condition that the texture features in the source texture image can be effectively captured and be subsequently used to constitute the target data set, then the centroids (prototypes), denoted as $\mathbf{V}_{\mathrm{S}} = [\mathbf{v}_{1,\mathrm{S}}, \cdots, \mathbf{v}_{C_{\mathrm{S}},\mathrm{S}}]^{\mathrm{T}}$, of all embedded clusters can conveniently be obtained using a certain conventional fuzzy clustering method. As disclosed in [47], the achieved $\mathbf{V}_{\mathrm{S}} = [\mathbf{v}_{1,\mathrm{S}}, \cdots, \mathbf{v}_{C_{\mathrm{S}},\mathrm{S}}]^{\mathrm{T}}$ can be regarded as the knowledge that is capable of depicting the substance of all textures in the source image. With these cluster centroids acting as the knowledge, we can benefit from two features: (1) A cluster centroid is also referred to as a cluster prototype in fuzzy clustering, which suffices to indicate its nice representability to one cluster, and also to all the affiliated objects in one cluster; (2) A cluster centroid is synthetically generated via reliable theories as well as rigorous procedures, which facilitates its robustness when facing nosy situations.

For the challenge of potential data heterogeneity between the source and target domains, as already mentioned, a mechanism with capability of flexibly controlling the referable degree between these two domains should be feasible to address. To this end, we present the following *knowledge-leveraged prototype transfer* (*KL-PT*) formulation.

A. The KL-PT mechanism—Let us first cope with a relatively simple scenario, i.e. the cluster numbers in the source and target domains are the same, denoted as C. Suppose $\mathbf{V}_{\mathrm{S}} = [\mathbf{v}_{1,\mathrm{S}}, \cdots, \mathbf{v}_{C,\mathrm{S}}]^{\mathrm{T}}$ and $\mathbf{V}_{\mathrm{T}} = [\mathbf{v}_{1,\mathrm{T}}, \cdots, \mathbf{v}_{C,\mathrm{T}}]^{\mathrm{T}}$ signify the cluster prototypes in the source and target domains, respectively. Then the formula of the *knowledge-leveraged prototype transfer* (*KL-PT*) mechanism can be expressed as

$$\min\left(\Lambda_{\mathrm{KL-PT}}(\mathbf{V}_{\mathrm{S}}, \mathbf{V}_{\mathrm{T}}) = \lambda \sum_{j=1}^{C} \left\|\mathbf{v}_{j,\mathrm{T}} - \mathbf{v}_{j,\mathrm{S}}\right\|^2\right) \quad (4)$$

where $\lambda \geq 0$ is the regularization coefficient.

Eq. (4) measures the total gap between the estimated cluster prototypes in the target domain and the referenced ones in the source domain. In the sense of texture image segmentation, here $\mathbf{V}_{\mathrm{T}}$ refers to the texture prototypes in the target image that need to be estimated by our own method, whereas $\mathbf{V}_{\mathrm{S}}$ signifies the texture prototypes in the source image that are given for reference. The parameter λ controls the overall, referable degree between $\mathbf{V}_{\mathrm{T}}$ in the target domain to $\mathbf{V}_{\mathrm{S}}$ in the source domain. The larger the value of λ, the greater the overall referable degree between $\mathbf{V}_{\mathrm{T}}$ and $\mathbf{V}_{\mathrm{S}}$ is, and the smaller the expected total difference between $\mathbf{V}_{\mathrm{T}}$ and $\mathbf{V}_{\mathrm{S}}$ is.

B. The knowledge-leveraged prototype matching (KL-PM) mechanism—KL-PT in the form of Eq. (4) assumes that the cluster numbers in the source and target domains are equal, which sometimes restricts its practicability. For example, the potential texture

numbers in Fig. 2 (a) and (c) are different: the former is 7 and the latter is 5. Key to this situation is to appropriately differentiate the importance of each cluster prototype in the source domain so as to correctly utilize them as the knowledge for transfer clustering in the target domain. To this end, adapting from [47], we introduce another transfer clustering mechanism termed *knowledge-leveraged prototype mat* ching (*KL-PM*), which can be formulated as

$$\min\left(J_{\mathrm{KL-PM}}(\mathbf{U}_{\mathrm{T}},\mathbf{P}_{\mathrm{T\&S}},\mathbf{V}_{\mathrm{T}})=\sum_{i=1}^{N_{\mathrm{T}}}\sum_{j=1}^{C_{\mathrm{T}}}\mu_{ij,\mathrm{T}}^{m_1}\left\|\mathbf{x}_{i,\mathrm{T}}-\mathbf{v}_{j,\mathrm{T}}\right\|^2+\beta\sum_{j=1}^{C_{\mathrm{T}}}\sum_{k=1}^{C_{\mathrm{S}}}p_{jk}^{m_2}\left\|\mathbf{v}_{j,\mathrm{T}}-\mathbf{v}_{k,\mathrm{S}}\right\|^2\right)$$

$$\text{s.t. } \mu_{ij}\in[0,1],\ \sum_{j=1}^{C_{\mathrm{T}}}\mu_{ij}=1,\ p_{jk}\in[0,1],$$

$$\sum_{k=1}^{C_{\mathrm{S}}}p_{jk}=1,\ 1\le i\le N_{\mathrm{T}},\ 1\le j\le C_{\mathrm{T}},\ 1\le k\le C_{\mathrm{S}} \quad (5)$$

in which the notations of $\mathbf{x}_{i,\mathrm{T}}$ ($i=1,\ldots,N_{\mathrm{T}}$) $\in X_{\mathrm{T}}$, $\mathbf{U}_{\mathrm{T}}$, $\mathbf{P}_{\mathrm{T\&S}}$, $\mathbf{V}_{\mathrm{T}}$, and $\mathbf{V}_{\mathrm{S}}$ are the same as those listed in Table 1. N_{T} denotes the data size in the target domain; C_{S} and C_{T} signify the cluster numbers in the source and target domains separately; $m_1>1$ and $m_2>1$ are two fuzzifiers controlling the model fuzziness; and $\beta>0$ is the regularization parameter.

Eq. (5) includes two terms. The first, originating from classical FCM, aims to divide the data in the target domain into C_{T} groups with overall minimum intra-cluster deviation as well as maximum inter-cluster separation. The second attempts to determine the appropriate values of p_{jk}, $1\le j\le C_{\mathrm{T}}$, $1\le k\le C_{\mathrm{S}}$, i.e. the matching degrees of cluster prototypes between the target and source domains.

By the Lagrange optimization, the updating equations of $\mathbf{v}_{j,\mathrm{T}}$, $\mu_{ij,\mathrm{T}}$, and p_{jk} in Eq. (5) can easily be derived as

$$\mathbf{v}_{j,T}=\frac{\sum_{i=1}^{N_{\mathrm{T}}}\mu_{ij,\mathrm{T}}^{m_1}\mathbf{x}_{i,\mathrm{T}}+\beta\sum_{k=1}^{C_{\mathrm{S}}}p_{jk}^{m_2}\mathbf{v}_{k,\mathrm{S}}}{\sum_{i=1}^{N_{\mathrm{T}}}\mu_{ij,\mathrm{T}}^{m_1}+\beta\sum_{k=1}^{C_{\mathrm{S}}}p_{jk}^{m_2}} \quad (6)$$

$$\mu_{ij,\mathrm{T}} = \frac{1}{\sum_{l=1}^{C_\mathrm{T}} \left(\frac{\left\| \mathbf{x}_{i,\mathrm{T}} - \mathbf{v}_{j,\mathrm{T}} \right\|^2}{\left\| \mathbf{x}_{i,\mathrm{T}} - \mathbf{v}_{l,\mathrm{T}} \right\|^2} \right)^{\frac{1}{m_1 - 1}}} \quad (7)$$

$$p_{jk} = \frac{1}{\sum_{l=1}^{C_\mathrm{S}} \left(\frac{\left\| \mathbf{v}_{j,\mathrm{T}} - \mathbf{v}_{k,\mathrm{S}} \right\|^2}{\left\| v_{i,\mathrm{T}} - \mathbf{v}_{l,\mathrm{S}} \right\|^2} \right)^{\frac{1}{m_2 - 1}}} \quad (8)$$

After the iterative procedure, two desired outcomes regarding the target domain are obtained. One is the current estimate of cluster centroids, $\mathbf{V}_\mathrm{T} = [\mathbf{v}_{1,\mathrm{T}}, \ldots, \mathbf{v}_{C_\mathrm{T},\mathrm{T}}]^\mathrm{T}$ in the target domain. As they still need to be refined in our method, we call them the *raw cluster prototypes* of the target domain and designate them as $\mathbf{V}_\mathrm{T}^\mathrm{r} = [\mathbf{v}_{1,\mathrm{T}}^\mathrm{r}, \cdots, \mathbf{v}_{C_\mathrm{T},\mathrm{T}}^\mathrm{r}]^\mathrm{T}$. The other outcome is the eventual matching degrees $\mathbf{P}_{\mathrm{T\&S}} = [p_{jk}]_{C_\mathrm{T} \times C_\mathrm{S}}$. Via these matching values, the appropriate pairwise relationships regarding the cluster prototypes in the source and target domains are achieved. Large values of p_{jk} indicate that the jth cluster prototype in the target domain strongly matches the kth one in the source domain.

Next, we continue discussing how to extract knowledge from the source domain, based on the matching degrees, $\mathbf{P}_{\mathrm{T\&S}}$, so as to implement knowledge transfer in the case of inconsistent cluster numbers between the source and target domains. Given our assumption that the data in the source domain are sufficient, which implies that the number of embedded clusters in the source domain are more than or at least equal to that in the target domain, two ways are available here, and we call them the so-called crisp and flexible forms, respectively. In either case, the C_T *cluster representatives*, denoted as $\tilde{\mathbf{V}}_\mathrm{S} = [\tilde{\mathbf{v}}_{1,\mathrm{S}}, \cdots, \tilde{\mathbf{v}}_{C_\mathrm{T},\mathrm{S}}]^\mathrm{T}$, are achieved in the source domain, and regarded as the final knowledge for transfer learning in the target domain.

a. The crisp form

In this case, for each $\mathbf{v}_{j,\mathrm{T}}^\mathrm{r} \in \mathbf{V}_\mathrm{T}^\mathrm{r}$ $(j = 1, \ldots C_\mathrm{T})$, i.e. each of the raw cluster prototypes in the target domain, we directly designate the cluster prototype in the source domain that owns the maximum matching degree to $\mathbf{v}_{j,\mathrm{T}}^\mathrm{r}$ as $\tilde{\mathbf{v}}_{j,\mathrm{S}} \in \tilde{\mathbf{V}}_\mathrm{S}$. Namely,

$$\tilde{\mathbf{v}}_{j,\mathrm{S}} = \mathbf{v}_{k',\mathrm{S}},\ k' = \arg\max_k \left(\left[p_{jk} \in \mathbf{P}_{\mathrm{T\&S}} \mid k \in [1, C_\mathrm{S}] \right] \right),\ \ j \in [1, C_\mathrm{T}],\ \ \tilde{\mathbf{v}}_{j,\mathrm{S}} \in \tilde{\mathbf{V}}_\mathrm{S},\ \ \mathbf{v}_{k',\mathrm{S}} \in \mathbf{V}_\mathrm{S}. \quad (9)$$

b. The flexible form

Here all of the $\tilde{\mathbf{v}}_{j,\mathrm{S}} \in \tilde{\mathbf{V}}_{\mathrm{S}}, j \in [1, C_{\mathrm{T}}]$, are synthetically generated by means of the weighted sums:

$$\tilde{\mathbf{v}}_{j,\mathrm{S}} = \sum_{k=1}^{C_{\mathrm{S}}} \left(p_{jk} \mathbf{v}_{k,\mathrm{S}} \right), \quad j \in [1, C_{\mathrm{T}}], \quad \tilde{\mathbf{v}}_{j,\mathrm{S}} \in \tilde{\mathbf{V}}_{\mathrm{S}}, \quad \mathbf{v}_{k,\mathrm{S}} \in \mathbf{V}_{\mathrm{S}}.. \quad (10)$$

That is, for each $\mathbf{v}^{\mathrm{r}}_{j,\mathrm{T}} \in \mathbf{V}^{\mathrm{r}}_{\mathrm{T}}$ $(j = 1, \ldots, C_{\mathrm{T}})$ in the target domain, in terms of $\mathbf{V}_{\mathrm{S}} = [\mathbf{v}_{1,\mathrm{S}}, \cdots, \mathbf{v}_{C_{\mathrm{S}},\mathrm{S}}]^{\mathrm{T}}$ as well as the matching degrees, $p_{jk}(k = 1,..., C_s)$, we synthesize a virtual product as the referable object in the source domain, via the strategy of the weighted sum.

So far, even if there is data inconsistency between the source and target domains, via the strategies of extracting the cluster representatives from the source domain as well as controlling the referable degree between these two domains, transfer clustering is now available for target texture image segmentation. Accordingly, the KL-PT mechanism in the form of Eq. (4) can be rewritten as

$$\min \left(J_{\mathrm{KL-PT}}(\tilde{\mathbf{V}}_{\mathrm{S}}, \mathbf{V}_{\mathrm{T}}) = \lambda \sum_{j=1}^{C_{\mathrm{T}}} \left\| \mathbf{v}_{j,\mathrm{T}} - \tilde{\mathbf{v}}_{j,\mathrm{S}} \right\|^2 \right). \quad (11)$$

That is, in the case of different cluster numbers between the source target domains, KL-PT substitutes the C_{T} cluster representatives, $\tilde{\mathbf{V}}_{\mathrm{S}} = [\tilde{\mathbf{v}}_{1,\mathrm{S}}, \cdots, \tilde{\mathbf{v}}_{C_{\mathrm{T}},\mathrm{S}}]^{\mathrm{T}}$, for the original cluster prototypes, $\mathbf{V}_{\mathrm{S}} = [\mathbf{v}_{1,\mathrm{S}}, \cdots, \mathbf{v}_{C_{\mathrm{S}},\mathrm{S}}]^{\mathrm{T}}$, for the knowledge transfer across domains.

3.2. The proposed KL-TFCM

A. The complete framework of KL-TFCM—Now, by means of the two knowledge transfer mechanisms—KL-PM in the form of Eq. (5) and KL-PT in the form of Eq. (11), and based on FCM, we can propose our novel clustering model, referred to as *knowledge-leveraged transfer fuzzy C-means (KL-TFCM)*, for texture image segmentation. The eventual formulation of KL-TFCM is:

$$\min\left(J_{\mathrm{KL-TFCM}}(\mathbf{U}_{\mathrm{T}},\mathbf{V}_{\mathrm{T}})=\sum_{i=1}^{N_{\mathrm{T}}}\sum_{j=1}^{C_{\mathrm{T}}}\mu_{ij,\mathrm{T}}^{m}\left\|\mathbf{x}_{i,\mathrm{T}}-\mathbf{v}_{j,\mathrm{T}}\right\|^{2}+\lambda\sum_{j=1}^{C_{\mathrm{T}}}\left\|\mathbf{v}_{j,\mathrm{T}}-\widetilde{\mathbf{v}}_{j,\mathrm{S}}\right\|^{2}\right)\quad(12)$$

$$\text{s.t. } i\in[1,N_{\mathrm{T}}],\ j\in[1,C_{\mathrm{T}}],\ \mu_{ij}\in[0,1],\ \sum_{j=1}^{C_{\mathrm{T}}}\mu_{ij}=1$$

$$\text{Case}-\text{c: }\widetilde{\mathbf{v}}_{j,\mathrm{S}}=v_{k',\mathrm{S}},\ k'=\arg\max_{k}\left(\left[p_{jk}\in\mathbf{P}_{\mathrm{T\&S}}\mid k\in[1,C_{S}]\right]\right)$$

$$\text{Case}-\text{f: }\widetilde{\mathbf{v}}_{j,\mathrm{S}}=\sum\nolimits_{k=1}^{C_{\mathrm{S}}}\left(p_{jk}\mathbf{v}_{k,\mathrm{S}}\right)$$

where, $\mathbf{x}_{i,\mathrm{T}}$ ($i = 1, \ldots, N_{\mathrm{T}}$) $\in X_{\mathrm{T}}$, $\widetilde{\mathbf{v}}_{j,\mathrm{S}} \in \widetilde{\mathbf{V}}_{\mathrm{S}}$, $\mathbf{v}_{k,\mathrm{S}} \in \mathbf{V}_{\mathrm{S}}$, $p_{jk} \in \mathbf{P}_{\mathrm{T\&S}}$, $\mathbf{U}_{\mathrm{T}}$, and $\mathbf{V}_{\mathrm{T}}$ are the same as those listed in Table 1, and C_{S}, C_{T}, N_{T}, and λ are the same as those in Eq. (4) or (5).

Eq. (12) is also composed of two terms. The first term aims at partitioning the target data into C_{T} groups with optimal intercluster purity, while the second is devoted to suitably and flexibly exploiting the final knowledge, $\widetilde{\mathbf{V}}_{\mathrm{S}} = [\widetilde{\mathbf{v}}_{1,\mathrm{S}}, \cdots, \widetilde{\mathbf{v}}_{C_{\mathrm{T}},\mathrm{S}}]^{\mathrm{T}}$, from the source domain. The parameter $\lambda \geq 0$ determines the referable degree across the two domains. Greater values of λ indicate that the target domain should learn much from the source domain, i.e. $\mathbf{V}_{\mathrm{T}}$ should be much closer to $\widetilde{\mathbf{V}}_{\mathrm{S}}$; conversely, smaller values of λ mean that the overall similarity between $\mathbf{V}_{\mathrm{T}}$ and $\widetilde{\mathbf{V}}_{\mathrm{S}}$ is not strongly enforced.

Once again, via the Lagrange optimization, the updating equations regarding cluster prototype $\mathbf{v}_{j,\mathrm{T}}$ and membership $\mu_{ij,\mathrm{T}}$ in Eq. (12) are also deduced:

$$\mathbf{v}_{j,\mathrm{T}}=\frac{\sum_{i=1}^{N_{\mathrm{T}}}\mu_{ij,\mathrm{T}}^{m}\mathbf{x}_{i,\mathrm{T}}+\lambda\widetilde{\mathbf{v}}_{j,\mathrm{S}}}{\sum_{i=1}^{N_{\mathrm{T}}}\mu_{ij,\mathrm{T}}^{m}+\lambda}\quad(13)$$

$$\mu_{ij,\mathrm{T}}=\frac{1}{\sum_{l=1}^{C_{\mathrm{T}}}\left(\frac{\left\|\mathbf{x}_{i,\mathrm{T}}-\mathbf{v}_{j,\mathrm{T}}\right\|^{2}}{\left\|\mathbf{x}_{i,\mathbf{T}}-\mathbf{v}_{l,\mathrm{T}}\right\|^{2}}\right)^{\frac{1}{m-1}}}.\quad(14)$$

It should be noted that KL-TFCM is proposed based on KL-PM and KL-PL and that KL-PM is always performed before KL-TFCM in the same target domain. Therefore, as mentioned in Section 3.1-B, the raw cluster prototypes, $\mathbf{V}_{\mathrm{T}}^{\mathrm{r}} = [\mathbf{v}_{1,\mathrm{T}}^{\mathrm{r}}, \cdots, \mathbf{v}_{C_{\mathrm{T}},\mathrm{T}}^{\mathrm{r}}]^{\mathrm{T}}$, achieved by KL-PM in

the target domain can be further refined in our subsequent procedure. For this purpose, we initialize $\mathbf{V}_T = \mathbf{V}_T^r$ at the beginning of the iterative optimization with respect to Eqs. (13) and (14).

Last but not least, to facilitate understanding, it is worth summarizing the complete framework of KL-TFCM developed for target texture image segmentation. As illustrated in Fig. 3, this complete framework involves three stages: knowledge extraction, knowledge matching, and knowledge utilization.

1. Stage I: Knowledge extraction

   In this stage, the texture features in the reference texture image are first extracted in order to compose the source domain data set X_S. Then, via classic FCM, the prototypes (centroids), $\mathbf{V}_S = [\mathbf{v}_{1,S}, \cdots, \mathbf{v}_{C_S,S}]^T$, of all embedded clusters (i.e. all contained textures) are obtained as the knowledge for reference in the target domain.

2. Stage II: Knowledge matching

   The texture features of the target texture image are used to compose the target domain data set X_T. By KL-PM in the form of Eq. (5), the currently estimated, raw cluster prototypes, $\mathbf{V}_T^r = [\mathbf{v}_{1,T}^r, \cdots, \mathbf{v}_{C_T,T}^r]^T$, in the target domain as well as the final matching degrees, $\mathbf{P}_{T\&S}$, between the source and target domains are obtained. Subsequently, in terms of $\mathbf{P}_{T\&S}$, and via the crisp or flexible form, the C_T cluster representatives, $\tilde{\mathbf{V}}_S = [\tilde{\mathbf{v}}_{1,S}, \cdots, \tilde{\mathbf{v}}_{C_T,S}]^T$, in the source domain can be attained. After that, the rewritten KL-PT knowledge transfer mechanism in the form of Eq. (11) becomes feasible.

3. Stage III: Knowledge utilization

   Based on the joint action of KL-PM and KL-PT in the form of Eq. (11), KL-TFCM is now available for target texture image segmentation, no matter whether there is the difference of cluster numbers between the source and target domains or not. In KL-TFCM, the cluster representatives, $\tilde{\mathbf{V}}_S = [\tilde{\mathbf{v}}_{1,S}, \cdots, \tilde{\mathbf{v}}_{C_T,S}]^T$, from the source domain are regarded as the final knowledge for transfer clustering in the target domain. Initializing $\mathbf{V}_T = \mathbf{V}_T^r$ and using Eqs. (14) and (13) alternately, the eventual partitions on X_T, i.e. the segmentation result of the target texture image, can be determined.

B. Detailed core algorithms

In light of the two ways for generating the cluster representatives, $\tilde{\mathbf{V}}_S = [\tilde{\mathbf{v}}_{1,S}, \cdots, \tilde{\mathbf{v}}_{C_T,S}]^T$, from the source domain, i.e. using the crisp or flexible form, we categorize KL-TFCM into two specific versions—KL-TFCM-c and KL-TFCM-f, corresponding to Eqs. (9) and (10), respectively. The detailed procedure is listed as follows

Algorithms

Knowledge-leveraged transfer fuzzy *C*-means clustering (KL-TFCM)-c/-f

Inputs: The target domain data set X_T constituted by extracting texture features from the target texture image; the source domain data set X_S composed of texture features from the referenced texture image; the cluster numbers C_T and C_S in the target and source domains, respectively; the convergence threshold ε; the fuzzifiers m, m_1, m_2 and parameters λ, β in Eq. (1), (5), or (12); and the maximum number of iterations *max_iter*

Outputs: The eventual partitions on X_T, i.e. the segmentation result of target texture image

Stage I: Knowledge extraction

Step I-1:

Set the iteration index $t = 1$, initialize the fuzzy memberships $\mu_{ij}^{(t)}$ in Eq. (1) and compute the cluster prototypes $\overline{\mathbf{v}}_i^{(t)}$, $i = 1, \ldots, C_S$, using Eq. (2) in the source domain X_S;

Step I-2:

Compute the fuzzy memberships $\mu_{ij}^{(t+1)}$, $i = 1, \ldots, C_S$, $j = 1, \ldots N_S$, using Eq. (3);

Step I-3:

Compute the cluster prototypes $\overline{\mathbf{v}}_i^{(t+1)}$, $i = 1, \ldots, C_S$, using Eq. (2);

Step I-4:

If $|J_{\mathrm{FCM}}^{(t+1)} - J_{\mathrm{FCM}}^{(t)}| < \varepsilon$ or $t > max\_iter$, go to Step I-5; otherwise, set $t = t + 1$ and go to Step I-2;

Step I-5;

Step I-5: Set the cluster prototypes $\mathbf{V}_S = \mathbf{V}^{(t+1)} = [\mathbf{v}_1^{(t+1)}, \ldots, \mathbf{v}_{C_S}^{(t+1)}]^T$ in the source domain X_S.

Stage II: Knowledge matching

Step II-1:

Set the iteration index $t = 1$, initialize the fuzzy memberships $\mu_{ij,T}^{(t)}$ and the matching degrees $p_{jk}^{(t)}$ in Eq. (5), and compute the cluster prototypes $\overline{\mathbf{v}}_{j,T}^{(t)}$, $j = 1, \ldots, C_T$, using Eq. (6) in the target domain X_T;

Step II-2:

Compute the fuzzy memberships $\mu_{ij,T}^{(t+1)}$, $i = 1, \ldots, N_T$, $j = 1, \ldots, C_T$, using Eq. (7);

Step II-3:

Compute the matching degrees $p_{jk}^{(t+1)}$, $j = 1, \ldots, C_T$, $k = 1, \ldots, C_S$, using Eq. (8);

Step II-4:

Compute the cluster prototypes $\overline{\mathbf{v}}_{j,T}^{(t+1)}$, $j = 1, \ldots, C_T$, using Eq. (6);

Step II-5:

If $|J_{\mathrm{KL-PM}}^{(t+1)} - J_{\mathrm{KL-PM}}^{(t)}| < \varepsilon$ or $t > max\_iter$, go to Step II-6; otherwise, set $t = t + 1$ and go to Step II-2;

Step II-6:

Set the raw cluster prototypes $\mathbf{V}_T^r = \mathbf{V}_T^{(t+1)} = [\mathbf{v}_{1,T}^{(t+1)}, \ldots, \mathbf{v}_{C_T,T}^{(t+1)}]^T$ and the final matching degrees $\mathbf{P}_{T\&S} = [p_{jk}^{(t+1)}]_{C_T \times C_S}$;

Step II-5: Generate the C_T cluster representatives, $\tilde{\mathbf{V}}_S = [\tilde{\mathbf{v}}_{1,S}, \cdots, \tilde{\mathbf{v}}_{C_T,S}]^T$, of the source domain as the final knowledge for the target domain, according to: *Case-c: the crisp form*, *i.e.* Eq. (9); *Case-f: the flexible form*, *i.e.* Eq. (10).

Stage III: Knowledge utilization

Step III-1: Set the iteration index $t = 1$, initialize the cluster prototypes $\mathbf{V}_{\mathrm{T}}^{(t)} = \mathbf{V}_{\mathrm{T}}^{\mathrm{r}} = [\mathbf{v}_{1,\mathrm{T}}^{\mathrm{r}}, \cdots, \mathbf{v}_{C_{\mathrm{T}},\mathrm{T}}^{\mathrm{r}}]^{\mathrm{T}}$ in Eq. (12), and compute the fuzzy memberships $\mu_{ij,\mathrm{T}}^{(t)}$ using (14) in the target domain X_{T};

Step III-2: Compute the cluster prototypes $\overline{\mathbf{v}}_{j,\mathrm{T}}^{(t+1)}$, $j = 1, \ldots, C_{\mathrm{T}}$, using (13);

Step III-3: Compute the fuzzy memberships $\mu_{ij,\mathrm{T}}^{(t+1)}$, $i = 1, \ldots, N_{\mathrm{T}}$, $j = 1, \ldots, C_{\mathrm{T}}$, using (14);

Step III-4: If $| J_{\mathrm{KL-TFCM}}^{(t+1)} - J_{\mathrm{KL-TFCM}}^{(t)} | < \varepsilon$ or $t > max\_iter$, go to Step III-5; otherwise, $t = t + 1$ and go to Step III-2;

Step III-5: The final memberships matrix $\mathbf{U}_{\mathrm{T}}$ in the target domain is achieved, i.e. $\mathbf{U}_{\mathrm{T}} = \mathbf{U}_{\mathrm{T}}^{(t+1)} = [\mu_{ij,T}^{(t+1)}]_{C_{\mathrm{T}} \times N_{\mathrm{T}}}$;

Step III-6: Determine the eventual partitions on the target texture image according to the eventual memberships $\mathbf{U}_{\mathrm{T}}$.

Let us analyse the computational cost of KL-TFCM in stages. The time complexity of the first stage is $O(ma\ x\_tria \cdot max\_iter \cdot (N_{\mathrm{S}} \cdot C_{\mathrm{S}} + C_{\mathrm{S}}))$, the second stage is $O(ma\ x\_tria \cdot max\_iter \cdot (N_{\mathrm{T}} \cdot C_{\mathrm{T}} + C_{\mathrm{T}} + C_{\mathrm{S}} \cdot C_{\mathrm{T}}))$, and the final stage is $O(ma\ x\_tria \cdot max\_iter \cdot (N_{\mathrm{T}} \cdot C_{\mathrm{T}} + C_{\mathrm{T}}))$, in which, max_tria and max_iter are, respectively, the maximal numbers of trials and iterations; N_{S} and N_{T} are separately the data sizes in the source and target domains; and C_{S} and C_{T} signify the cluster numbers of the source and target domains, respectively.

4. Experimental studies

4.1. Setup

In this section, we focus on evaluating the real-world segmentation performance of texture images of our research. In addition to KL-TFCM-c and KL-TFCM-f, eight other correlative algorithms are enlisted for performance comparison, including classic FCM, STC [31], TSC [32], LSSMTC [49], CombKM [49], DRCC [51], CKM [53], and SFCM [58]. All of these competitive algorithms have been briefly introduced in Section II, except for CombKM. As described in [49], CombKM refers to the K-means performed on the combined data set constituted by merging the data of all tasks together. These algorithms are good representatives of the state-of-the-art approaches associated with our research. Among these, FCM, SFCM, KL-TFCM-c, and KL-TFCM-f belong to fuzzy clustering; KL-TFCM-c, KL-TFCM-f, STC, and TSC belong to transfer clustering; Both STC and TSC also belong to co-clustering; LSSMTC and CombKM belong to multi-task clustering; and DRCC, CKM, and SFCM are, respectively, the member of co-clustering, semi-supervised clustering, and supervised clustering.

For measuring the clustering effectiveness of these involved approaches, two well-accepted validity metrics, i.e. NMI (Normalized Mutual Information) [48] and RI (Rand Index) [48], are employed. Both NMI and RI take values within the interval [0,1]. The greater the value of NMI or RI, the better performance the corresponding algorithm indicates. Their definitions are briefly reviewed as follows.

$$NMI = \frac{\sum_{i=1}^{C}\sum_{j=1}^{C} N_{i,j} \log N \cdot N_{i,j}/N_i \cdot N_j}{\sqrt{\sum_{i=1}^{C} N_i \log N_i/N \cdot \sum_{j=1}^{C} N_j \log N_j/N}} \quad (15)$$

where $N_{i,j}$ is the number of agreements between cluster i and class j, N_i is the number of data points in cluster i, N_j is the number of data points in class j, and N signifies the data capacity of the whole dataset.

$$RI = \frac{f_{00} + f_{11}}{N(N-1)/2} \quad (16)$$

where f_{00} denotes the number of any two sample points belonging to two different clusters, f_{11} denotes the number of any two sample points belonging to the same cluster, and N is the number of all the sample points.

The grid search strategy [48] was enlisted for partial parameter settings during our experiments. The values or trial ranges of core parameters involved in the recruited algorithms are listed in Tables 2 and 3. The experimental results of matching approaches are reported in terms of the means and standard deviations of NMI and RI after twenty times of random initialization based running on the target data sets.

All of our experiments were implemented via MATLAB 2010b on a PC with Intel i5-3317 U 1.70 GHz CPU and 16GB RAM.

4.2. Texture image segmentation

A. Constitution of the transfer Scenarios of Texture Image Segmentation—For constituting the experimental texture images, the well-known *Brodatz texture* [59] repository was enlisted in our research. Specifically, thirteen basic textures: D3, D6, D21, D31, D33, D41, D45, D49, D53, D56, D93, D96, and D101, in this repository were used to synthesize the texture images acting as the source or target domains for transfer clustering in our experiments.

It should be noted that, for achieving the balance of good readability and appropriate paper length, we show our experimental studies in two parts: the major contents are shown in Section IV and the others are given in the Appendix as supplementary material.

To perform our experiments, we have first generated two data scenarios suitable for transfer clustering, as illustrated in Figs. 4 and A1, respectively. Specifically, for transfer learning, TI_S1, Fig. 4 (a), was enlisted as the only source domain and TI_T1_1 to TI_T1_8, Fig. 4 (b)–(i), as the target domains respectively. All these synthetic texture images were rescaled to 100 × 100 resolution, and to some of them the Gaussian noise with different standard

deviations was added in order to simulate multiple noisy data situations. In our experiments, *TI-T*1_1 to *TI-T*1_8 (i.e. Fig. 4 (b)–(i)) belong to two types of target domains. That is, each of *TI-T*1_1 to *TI-T*1_4 owns the same texture number as that in *TI-S*1 (i.e. 7 clusters), but has an inconsistent data distribution, whereas the numbers of clusters in *TI-T*1_5 to *TI-T*1_8 are 3, 4, 5, and 6, respectively, which are all different from that in *TI-S*1. In addition, the noise amplitudes in these target domain images are also different. For example, the standard deviations of Gaussian noise in *TI-T*1_1, *TI-T*1_4, and *TI-T*1_5 to *TI-T*1_8 are 0.1, while in *TI-T*1_2 and *TI-T*1_3 are 0.2 and 0, respectively. Please refer to Fig. 4 for the details regarding the texture arrangement, cluster number, and noise level in each target texture image. The situations are similar in Fig. A1 in which *TI_T*2_1, *TI_T*2_2, and *TI_S*2 all have 7 clusters, whereas *TI_T*2_3 to *TI_T*2_6 have from 3 to 6 clusters. These two transfer scenarios enable us to extensively investigate the performance of all employed algorithms in the realistic applications of target texture image segmentation.

The Gabor filter [60] was used to extract intrinsic texture features of all texture images in terms of the filtering bank with 6 orientations (at every 30°) and 5 frequencies (starting from 0.46). As such, the data sets corresponding to all texture images were produced, with the data dimensionality and data size being 30 and 10,000, respectively. Note that for the purpose of good readability, we use consistent nomenclature designating these data sets as the names of their associated texture images.

B. Comparisons of segmentation results—The ideal segmentation results regarding all target texture images are first illustrated in Figs. 5 and A2, respectively, where the small squares with the same colors in each subfigure signify the same textures which should be grouped into the same clusters.

In contrast, the actual segmentation results as well as the scores of NMI and RI achieved by the ten competitors are shown in Figs. 6, 7, A3, and A4 and Tables 4 and A1. Based on these outcomes, we make the following observations.

1. Transfer clustering using the same number of clusters but with inconsistent data distributions in the source and target domains:
    i. Due to the existing noise interference, classic FCM did not obtain acceptable clustering effectiveness and segmentation results on any noisy images, e.g., *TI_T*1_1, *TI_T*1_2, *TI_T*1_4, *TI_T*2_1, and *TI_T*2_2. Conversely, benefiting from the reference information across the source and target domains, all of the transfer clustering algorithms, i.e. STC, TSC, KL-TFCM-c, and KL-TFCM-f, obtain relatively good performance on *TI_T*1_1 to *TI_T*1_4 and *TI_T*2_1 to *TI_T*2_2, compared with the other non-transfer-clustering algorithms. This demonstrates the merit of transfer clustering in the practice of target texture image segmentation.
    ii. As far as the transfer clustering approaches are concerned, the clustering effectiveness as well as the segmentation performance of both KL-TFCM-c and KL-TFCM-f on real-world data are better than

those of STC and TSC in all of the noisy data conditions, except on *TI_T*1_3 (i.e. Fig. 4 (d)) where the data are never distorted by noise. KL-TFCM-c and KL-TFCM-f rank Nos. 2 and 3, respectively, and are only a little worse than STC. This distinctly reflects the superiority regarding our KL-PM and KL-PT based three stages of knowledge transfer, i.e. knowledge extraction, knowledge matching, and knowledge utilization. As such, regardless of the data distribution diversities in the source and target images, the knowledge from the source domain, i.e. the texture characteristics in *TI_S*1 and *TI_S*2 can be extensively, appropriately referenced by KL-TFCM-c/-f on the target domain images. This is consequently conducive for them to having insights into the ground truth of texture characteristics in these target images, even if these images were distorted by noise. That is, with the self-adaptive knowledge reference from the source domain, both KL-TFCM-c and KL-TFCM-f demonstrate excellent anti-noise properties.

iii. Comparing KL-TFCM-c/-f with the multi-task and co-clustering algorithms: CombKM, LSSMTC, and DRCC, our KL-TFCM-c/-f algorithms are also superior on all target images due to their different mechanisms. More specifically, because of the existing noise interference as well as the potential data distribution diversities between the target and source domains, the raw data in the source domain could not directly provide valuable information to the target domain data. As evidence of this, CombKM and LSSMTC, two multi-task clustering methods directly utilizing the raw data in the source domain, were prone to encountering unexpectedly negative interactions between tasks instead of both gaining performance improvements. DRCC, one of pure co-clustering approaches, was devoted to constructing the manifold structures on both data instances and features, and then to simultaneously smoothing these two types of manifolds. However, DRCC generally did not achieve relatively satisfactory clustering and segmentation performance throughout all experiments, probably due to its sensitivity to our adopted strategy with respect to texture feature extraction. On the contrary, with the cluster prototypes rather than the raw data in the source domain acting as the reference in the target domain, both KL-TFCM-c and KL-TFCM-f exhibit more robust clustering effectiveness than do the other methods. This demonstrates the significance of our own work.

iv. CKM was enlisted as the representative of semi-supervised clustering in our experiments, and SFCM of supervised clustering. To perform CKM, we randomly selected 100 labeled examples from the source domain and converted them into the pairwise constraints as the supervision. As for SFCM, all examples along with their labels in the source domain were used to train the parameterized distance measure for fuzzy clustering, and then we used this distance measure with the

learned parameters to group the data in the target domain. However, as could be predicted, neither CKM nor SFCM worked well when facing such two domains having distinctly different data distributions. Due to the data inconsistency between the source and target domains, in CKM, many of the 100 selected examples from the source domain equaled essentially to outliers to the data in the target domain, which decreased the performance of CKM instead of facilitating clustering. In SFCM, likewise, because of the data inconsistency across two domains, the learned distance measure in the source domain became inapplicable in the target domains. This incurred the overall inefficiency of SFCM in nearly all of the transfer data scenes.

2. Transfer clustering when source and target domains have different numbers of clusters:

   i. *TI_T*1_*5* to *TI_T*1_*8* (Fig. 4 (f)–(i)) and *TI_T*2_3 to *TI_T*2_6 (Fig. A1 (d)–(g)) were used to further verify the effectiveness and reliability of our approach for handling another type of data heterogeneity existing in transfer learning: differences in the numbers of clusters and in the data distributions between the source and target domains. In such cases, LSSMTC, CDRCC, SFCM, STC, and TSC, cannot be applied, as they strictly require the cluster number consistency between the source and target domains. In contrast, our proposed KL-TFCM-c and KL-TFCM-f approaches are applicable for such situations and, compared with classic FCM, CombKM, and CKM, both of them achieved quite considerable performance improvements. This indicates, again, that the proposed, three-stage-interlinked knowledge transfer framework in our research is effective at coping with the data inconsistency between the source and target domains, and accordingly facilitating the clustering of both KL-TFCM-c and KL-TFCM-f on target texture images.

   ii. When KL-TFCM-c and KL-TFCM-f are compared only with each other, their performance differences are evident which, how46 ever, is not notable in the cases of the first type of transfer clustering. Specifically, KL-TFCM-f generally features better clustering performance versus KL-TFCM-c on all of *TI_T*1_5 to *TI_T*1_8 and *TI_T*2_3 to *TI_T*2_6. This implies that, for generating the cluster representatives, $\tilde{\mathbf{V}}_S = [\tilde{\mathbf{v}}_{1,S}, \cdots, \tilde{\mathbf{v}}_{C_T,S}]^T$, of the source domain in our work, the strategy of weighted sum, i.e. the so-called flexible form (see Eq. (10)), appears more efficient than the maximum matching strategy, namely, the crisp form (see Eq. (9)), when the numbers of clusters in the source and target domains are different.

All of these experimental results indicate that, our proposed, three-stage-based transfer clustering algorithms—KL-TFCM-c and KL-TFCM-f, generally feature better clustering and segmentation performance than many existing, popular clustering methods in both two types of texture image segmentation, i.e. one possesses the same cluster number but different

data distributions in the source and target domains, while the other has inconsistent cluster numbers between the two domains. In addition, KL-TFCM-f appears more effective and reliable than KL-TFCM-c in the latter case.

5. Conclusions

Motivated by target texture image segmentation, we propose the three-stage-based transfer clustering framework as well as the two corresponding algorithms designated as KL-TFCMc and KL-TFCM-f. Two embedded, dedicated knowledge transfer mechanisms—KL-PT and KL-PM are simultaneously designed. KL-PT provides the way to flexibly learn the valuable knowledge even in the presence of noise in the source domain. KL-PM is devoted to mining the appropriate pairwise relationships of clustering prototypes between the source and target domains even if their numbers of clusters are different. Benefiting from the joint action of KL-PT and KL-PM, and via the three-stage-interlinked knowledge transfer, both KL-TFCM-c and KL-TFCM-f generally feature preferable clustering effectiveness and segmentation performance on almost all of the involved target texture images. As far as our KL-TFCM-c and KL-TFCM-f are concerned, due to the more flexible, efficient mechanism for generating the cluster representatives from the source domain, the latter performs better than the former in the case of different cluster numbers between the source and target domains.

In the future, two aspects of work are worth continuing. One is the more practical mechanism regarding parameter settings. The grid search strategy is now used in our work to determine the optimal values of parameters via two well-established validity indices: NMI and RI. Both of them are label-dependent [61]. From the viewpoint of practicability, a novel validity index independent of any label information will be perused in our future research. The other is the multiple source domains based knowledge transfer mechanism for fuzzy clustering which, in our opinion, is a very promising prospect.

Acknowledgments

This work was supported in part by the National Natural Science Foundation of China under Grants 61572236 and 61673194, by Natural Science Foundation of Jiangsu Province under Grant BK20160187, by the R&D Frontier Grant of Jiangsu Province under Grant BY2013015-02, and by the Fundamental Research Funds for the Central Universities under Grants JUSRP51614A and JUSRP11737. Research reported in this publication was also supported by National Cancer Institute of the National Institutes of Health, USA, under award number R01CA196687. The content is solely the responsibility of the authors and does not necessarily represent the official views of the National Institutes of Health, USA.

In addition, we would like to thank Bonnie Hami, MA (USA) for her editorial assistance in the preparation of this manuscript.

References

1Zhu L, Chung FL, Wang ST. Generalized fuzzy *C*-means clustering algorithm with improved fuzzy partitions. IEEE Trans Syst, Man, Cybern, Part B. 2009; 39(3):578–591.

2Jiang Y, Chung FL, Wang S. Enhanced fuzzy partitions vs data randomness in FCM. J Intell Fuzzy Syst. 2014; 27(4):1639–1648.

3Wang L, Pan C. Robust level set image segmentation via a local correntropy--based K-means clustering. Pattern Recognit. 2014; 47(5):1917–1925.

4Kim S, Yoo CD, Nowozin S, Kohli P. Image segmentation using higher-order correlation clustering. IEEE Trans Pattern Anal Mach Intell. 2014; 6(9):1761–1774.

5Ji Z, Liu J, Cao G, Sun Q, Chen Q. Robust spatially constrained fuzzy c-means algorithm for brain MR image segmentation. Pattern Recognit. 2014; 47(7):2454–2466.

6Bezdek JC. Pattern Recognition With Fuzzy Objective Function Algorithms Plenum Press; New York: 1981

7Havens TC, Bezdek JC, Leckie C, Hall LO, Palaniswami M. Fuzzy c-means algorithms for very large data. IEEE Trans Fuzzy Syst. 2012; 20(6):1130–1146.

8Wu J, Xiong H, Liu C, Chen J. A generalization of distance functions for fuzzy c-means clustering with centroids of arithmetic means. IEEE Trans Fuzzy Syst. 2012; 20(3):557–571.

9Ma J, Tian D, Gong M, Jiao L. Fuzzy clustering with non-local information for image segmentation. Int J Mach Learn Cybern. 2014; 5(6):845–859.

10Wang J, Wang S, Chung F, Deng Z. Fuzzy partition based soft subspace clustering and its applications in high dimensional data. Inform Sci. 2013; 246:133–154.

11Jiang Y, Chung FL, Wang S, Deng Z, Wang J, Qian P. Collaborative fuzzy clustering from multiple weighted views. IEEE Trans Cybern. 2015; 45(4):688–701. [PubMed: 25069132]

12Huang HC, Chuang YY, Chen CS. Multiple kernel fuzzy clustering. IEEE Trans Fuzzy Syst. 2012; 20(1):120–134.

13Pedrycz W. Collaborative fuzzy clustering. Pattern Recognit Lett. 2002; 23(14):1675–1686.

14Pedrycz W. Fuzzy clustering with a knowledge-based guidance. Pattern Recognition Lett. 2004; 25(4):469–480.

15Chung FL, Wang ST, Deng ZH, Chen S, Hu DW. Clustering analysis of gene expression data based on semi-supervised visual clustering algorithm. Soft Comput. 2006; 10(11):981–993.

16Pan SJ, Yang Q. A survey on transfer learning. IEEE Trans Knowl Data Eng. 2010 Oct; 22(10): 1345–1359.

17Lu J, Behbood V, Hao P, Zuo H, Xue S, Zhang G. Transfer learning using computational intelligence: a survey. Knowl-Based Syst. 2015; 80:14–23.

18Tao JW, Chung F-L, Wang ST. On minimum distribution discrepancy support vector machine for domain adaptation. Pattern Recognit. 2012; 45(11):3962–3984.

19Sun Z, , Chen YQ, , Qi J, , Liu JF. Adaptive localization through transfer learning in indoor Wi-Fi environment. Proceedings of 7th International Conference on Machine Learning and Applications; 2008 331336

20Bickel S, , Brückner M, , Scheffer T. Discriminative learning for differing training and test distributions. Proceedings of 24th International Conference on Machine Learning; 2007 8188

21Gao J, , Fan W, , Jiang J, , Han J. Knowledge transfer via multiple model local structure mapping. Proceedings of 14th ACM SIGKDD International Conference on Knowledge Discovery and Data Mining; 2008 283291

22Qian P, Jiang Y, Deng Z, Hu L, Sun S, Wang S, Muzic RF Jr. Cluster Prototypes and Fuzzy Memberships Jointly Leveraged Cross-Domain Maximum Entropy Clustering. IEEE Trans Cybern. 2016; 46(1):181–193. [PubMed: 26684257]

23Deng ZH, Jiang YZ, Chung FL, Ishibuchi H, Wang ST. Knowledge-Leverage based fuzzy system and its modeling. IEEE Trans Fuzzy Syst. 2013; 21(4):597–609.

24Deng Z, Choi K-S, Jiang Y, Wang S. Generalized hidden-mapping ridge regression, knowledge-leveraged inductive transfer learning for neural networks, fuzzy systems and kernel methods. IEEE Trans Cybern. 2014; 44(12):2585–2599. [PubMed: 24710838]

25Dong A, Chung F-L, Deng Z, Wang S. Semi-supervised SVM with extended hidden features. IEEE Trans Cybern. 2015; doi: 10.1109/TCYB.2015.2493161

26Yang P, , Tan Q, , Ding Y. Bayesian task-level transfer learning for non-linear regression. Proceedings of International Conference on Computer Science and Software Engineering; 2008 6265

27Mao W, Yan G, Bai J, Li H. Regression transfer learning based on principal curve. Lect Note Comput Sci. 2010; 6063:365–372.

28Deng Z, Jiang Y, Choi KS, Chung FL, Wang S. Knowledge-leveraged TSK fuzzy system modeling. IEEE Trans Neural Netw Learn Syst. 2013; 24(8):1200–1212. [PubMed: 24808561]

29Wang Z, Song YQ, Zhang CS. Transferred dimensionality reduction. Lect Notes Comput Sci. 2008; 5212:550–565.

30Pan SJ, Kwok JT, Yang Q. Transfer learning via dimensionality reduction. Proc AAAI'08. 2008; 2:677–682.

31Dai W, Yang Q, Xue G, Yu Y. Self-taught clustering. Proc 25th Int Conf Machine Learning. 2008:200–207.

32Jiang WH, , Chung FL. Machine Learning and Knowledge Discovery in Databases Springer; Berlin Heidelberg: 2012 Transfer spectral clustering; 789803

33Liao X, , Xue Y, , Carin L. Logistic regression with an auxiliary data source. Proceedings of 21st Int'l Conference on Machine Learning; 2005 505512

34Huang J, , Smola A, , Gretton A, , Borgwardt KM, , Schölkopf B. Correcting sample selection bias by unlabeled data. Proceedings of 19th Annual Conference on Neural Information Processing Systems; 2007

35Rosenstein MT, , Marx Z, , Kaelbling LP. To transfer or not to transfer. Proceedings of Conference on Neural Information Processing Systems (NIPS '05) Workshop Inductive Transfer: 10 Years Later; 2005 Dec;

36Raina R, , Battle A, , Lee H, , Packer B, , Ng AY. Self-taught learning: transfer learning from unlabeled data. Proceedings of 24th Int'l Conference on Machine Learning; 2007 759766

37Jebara T. Multi-task feature and kernel selection for SVMs. Proceedings of 21st Int'l Conference on Machine Learning; 2004 July;

38Mihalkova L, , Huynh T, , Mooney RJ. Mapping and revising Markov logic networks for transfer learning. Proceedings of 22nd Association for the Advancement of Artificial Intelligence (AAAI) Conference on Artificial Intelligence; 2007 608614

39Evgeniou T, , Pontil M. Regularized multi-task learning. Proceedings of the 10th ACM SIGKDD Int'l Conference on Knowledge Discovery and Data Mining; 2004 109117

40Daumé H, III. Frustratingly easy domain adaptation. Proceedings of the 45th Annual Meeting of the Associations for Computational Linguistics; 2007 256263

41Ben-David S, , Blitzer J, , Crammer K, , Pereira F. Analysis of representations for domain adaptation. Proceedings 20th Annual Conference on Neural Information Processing Systems; 2007 137144

42Blitzer J, , McDonald R, , Pereira F. Domain adaptation with structural correspondence learning. Proceedings of Conference on Empirical Methods in Natural Language; 2006 120128

43Miyamoto S, , Ichihashi H, , Honda K. Algorithms For Fuzzy Clustering Springer; 2008

44Wang S, Chung KL, Deng Z, et al. Robust maximum entropy clustering with its labeling for outliers. Soft Compt. 2006; 10(7):555–563.

45Miyamoto S, , Umayahara K. Fuzzy clustering by quadratic regularization. Proceedings of the 1998 IEEE International Conference on Fuzzy Systems and IEEE World Congress on Computational Intelligence; 1998 13941399

46Krishnapuram R, Keller M. A possibilistic approach to clustering. IEEE Trans Fuzzy Syst. 1993; 1(2):98–110.

47Deng Z, Jang Y, Chung F-L, Ishibuchi H, Choi K-S, Wang S. Transfer prototype-based fuzzy clustering. IEEE Trans Fuzzy Syst. 2016; 24(5):1210–1232.

48Deng Z, Choi KS, Chung FL, Wang S. Enhanced soft subspace clustering integrating within-cluster and between-cluster information. Pattern Recognit. 2010; 43(3):767–781.

49Gu QQ, , Zhou J. Learning the shared subspace for multi-task clustering and transductive transfer classification. Proceedings of the 9th IEEE International Conference on Data Mining; 2009 159168

50Zhang Z, Zhou J. Multi-task clustering via domain adaptation. Pattern Recognit. 2012; 45(1):465–473.

51Gu QQ, , Zhou J. Co-clustering on manifolds. Proceedings of the 15th International Conference on KDD; 2009 359368

52Dhillon IS, , Mallela S, , Modha DS. Information-theoretic co-clustering. Proceedings of the 9th ACM SIGKDD Int. Conf. on KDD'03; 2003 8998

53Wagstaff K, , Cardie C, , Rogers S, , Schrödl S. Constrained k-means clustering with background knowledge. Proceedings of the Eighteenth International Conference on Machine Learning; 2001 577584

54Xing EP, , Ng AY, , Jordan M, , Russell S. Advances in Neural Information Processing Vol. 15. MIT Press; 2003Distance metric learning, with application to clustering with side-information.

55Klein D, , Kamvar SD, , Manning C. From instance-level constraints to space-level constraints: making the most prior knowledge in data clustering. Proc. ICML'02; Sydney, Australia. 2002

56Finley T, , Joachims T. Supervised clustering with support vector machines. Proceedings of the Twenty-second International Conference on Machine Learning; 2005 217224

57Finley T, Joachims T. Supervised k-means clustering. Cornell Computing and Information Science. 2008:1813–11621.

58Abonyi J, Szeifert F. Supervised fuzzy clustering for the identification of fuzzy classifiers. Pattern Recognit Lett. 2003; 24:2195–2207.

59Randen T. Brodatz Texture http://www.ux.uis.no/~tranden/brodatz.html

60Kyrki V, Kamarainen JK, Kalviainen H. Simple Gabor feature space for invariant object recognition. Pattern Recognit Lett. 2004; 25(3):311–318.

61Desgraupes B. Clustering Indices University Paris Ouest, Lab Modal'X; 2013

Appendix

Table A1

Performance comparisons of ten involved algorithms on *TI_T2_1* to *TI_T2_6*.

Data sets	Validity Metrics	FCM	LSSMTC	CombKM	DRCC	CKM	SFCM	STC	TSC	KL-TFCM-c	KL-TFCM-f
TI_T2_1	NMI-mean	0.0670	0.1250	0.0491	0.1745	0.1572	0.1812	0.2593	0.2723	**0.3444**	0.3372
	NMI-std	0.0033	0.0217	0.0020	0.0221	0.0056	0.0083	0.0213	0.0059	0.0062	0.0095
	RI-mean	0.7501	0.6545	0.5101	0.6901	0.7671	0.6898	0.7979	0.8000	**0.8158**	0.8111
	RI-std	0.0051	0.0108	0.0339	0.0045	0.0036	0.0125	0.0072	0.0023	0.0057	0.0090
TI_T2_2	NMI-mean	0.0217	0.0903	0.0330	0.1016	0.1190	0.1061	0.2077	0.2403	0.2804	**0.2839**
	NMI-std	0.0011	0.0014	0.0037	0.0086	0.0152	0.0067	0.0073	0.0041	0.0227	0.0199
	RI-mean	0.7422	0.7015	0.5855	0.7147	0.7543	0.6831	0.7830	0.7845	0.7958	**0.7984**
	RI-std	0.0012	0.0059	0.0033	0.0134	0.0037	0.0178	0.0024	0.0082	0.0113	0.0087
TI_T2_3	NMI-mean	0.3207	–	0.4122	–	0.1201	–	–	–	0.4685	**0.5036**
	NMI-std	0.0100	–	0.0008	–	0.0167	–	–	–	0.0002	0
	RI-mean	0.6977	–	0.7542	–	0.6042	–	–	–	0.7757	**0.7886**
	RI-std	0.0066	–	0.0006	–	0.0123	–	–	–	0.0001	0
TI_T2_4	NMI-mean	0.1005	–	0.3032	–	0.1355	–	–	–	0.3755	**0.4179**
	NMI-std	0.0146	–	0.0023	–	0.0046	–	–	–	0.0173	0.0005
	RI-mean	0.6564	–	0.7104	–	0.6660	–	–	–	0.7448	**0.7633**
	RI-std	0.0063	–	0.0011	–	0.0019	–	–	–	0.0058	0.0001
TI_T2_5	NMI-mean	0.1249	–	0.2691	–	0.1597	–	–	–	0.3081	**0.3465**
	NMI-std	0.0077	–	0.0124	–	0.0067	–	–	–	0.0449	0.0150
	RI-mean	0.7052	–	0.7378	–	0.7064	–	–	–	0.7587	**0.7623**
	RI-std	0.0049	–	0.0158	–	0.0089	–	–	–	0.0224	0.0082
TI_T2_6	NMI-mean	0.1727	–	0.3022	–	0.1846	–	–	–	0.3419	**0.3851**
	NMI-std	0.0078	–	0.0131	–	0.0249	–	–	–	0.0216	0.0069
	RI-mean	0.7394	–	0.7677	–	0.7393	–	–	–	0.7877	**0.7938**
	RI-std	0.0069	–	0.0361	–	0.0052	–	–	–	0.0076	0.0008

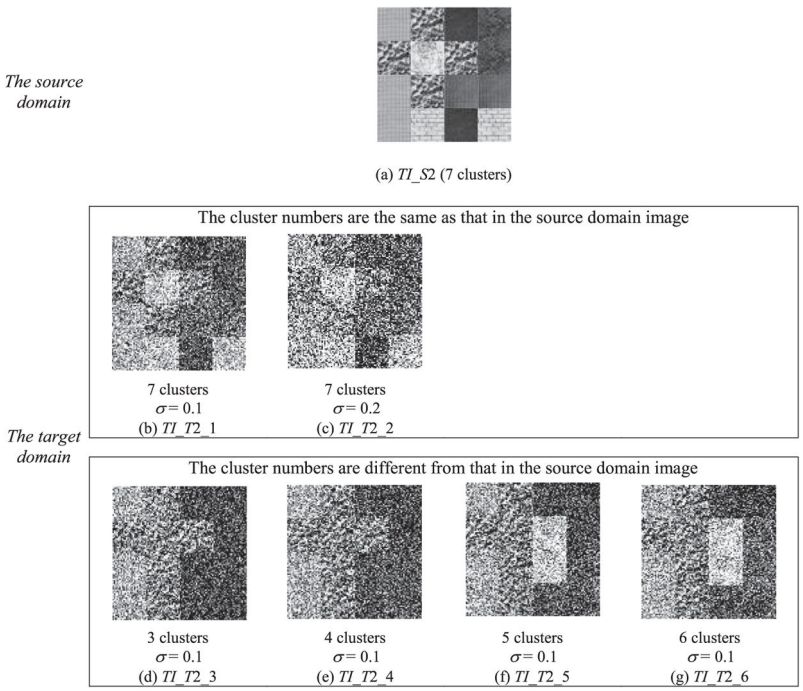

Fig. A1.

Artificial scenario 2 for transfer clustering. (a) *TI_S*2: the image acting as the source domain; (b)–(c) *TI_T*2_1 to *TI_T*2_2: the target domain images owning the same cluster number as that in *TI_S*2, but different distributions; (d)–(g) *TI_T*2_3 to *TI_T*2_6: the target domain images whose cluster numbers are different from that of *TI_S*2.

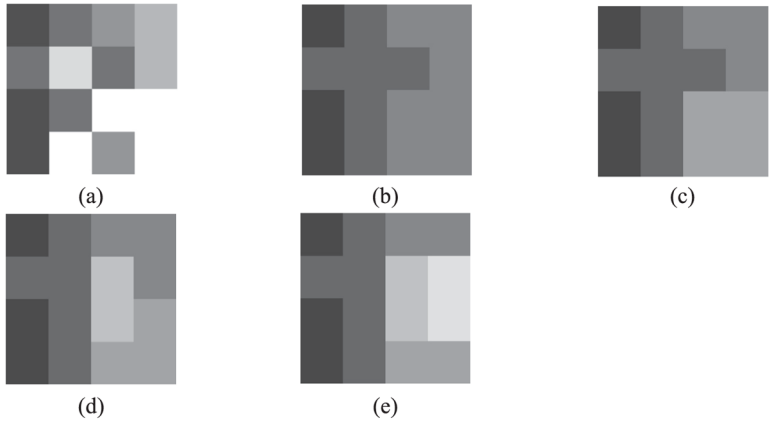

Fig. A2.

Illustrations of ideal segmentation of employed texture images. (a) for *TI_T*2_1 and *TI_T*2_2; (b) for *TI_T*2_3; (c) for *TI_T*2_4; (d) for *TI_T*2_5; (e) for *TI_T*2_6.

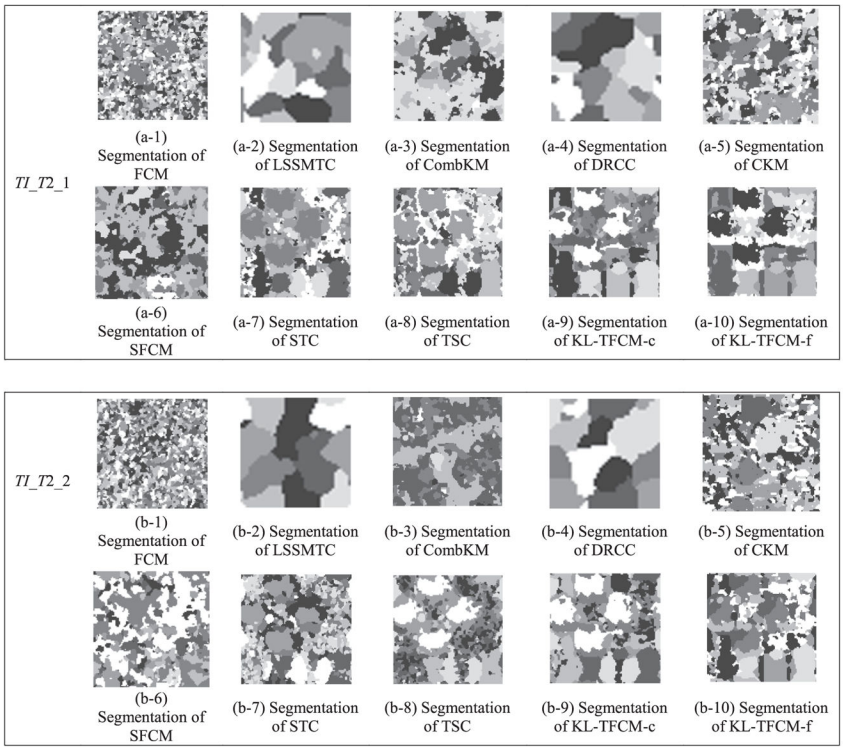

Fig. A3.

Segmentation results of ten clustering approaches on target texture images *TI_T*2_1 to *TI_T*2_2.

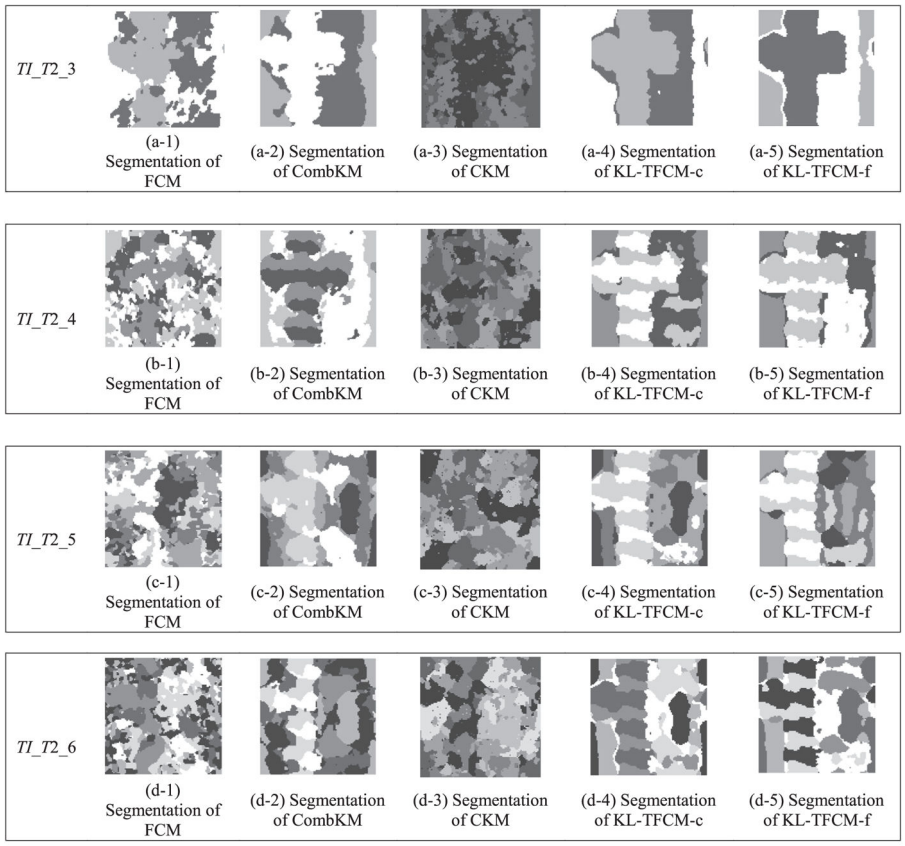

Fig. A4.

Segmentation results of five clustering approaches on target texture images *TI_T2*_3 to *TI_T2*_6.

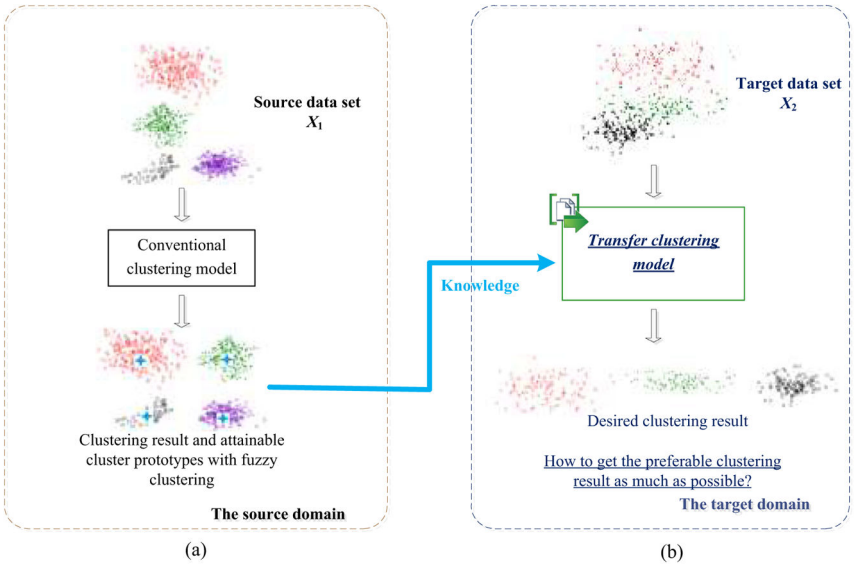

Fig. 1.
Outline of knowledge-leveraged transfer clustering.

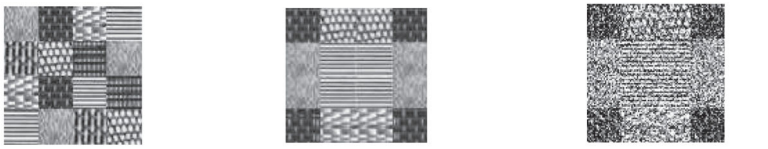

(a) the referenced texture image (7 textures)

(b) the essence of the target texture image (5 textures)

(c) the target texture image distorted by noise (5 textures)

Fig. 2.

Illustration of transfer clustering occurred in texture image segmentation.

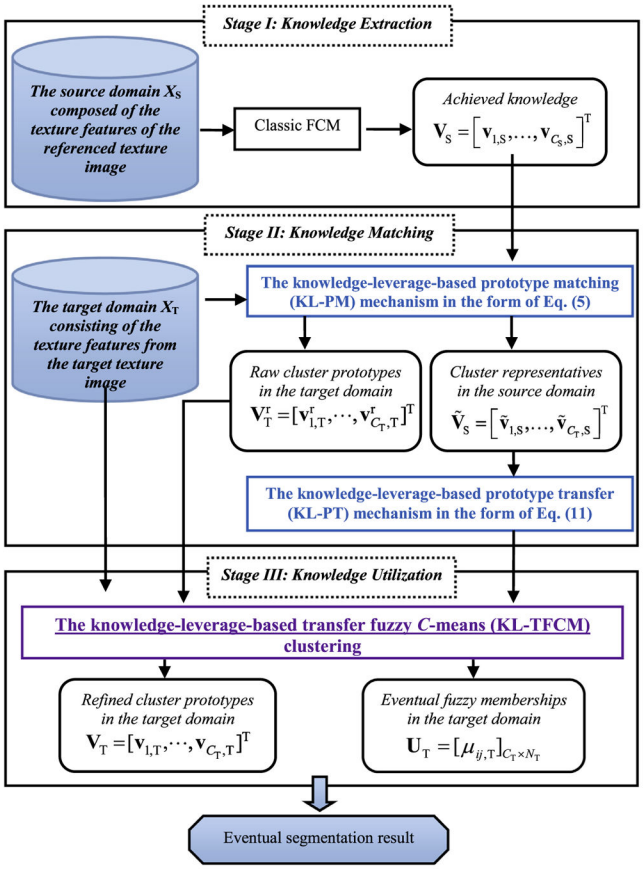

Fig. 3.
Complete framework of KL-TFCM for texture image segmentation.

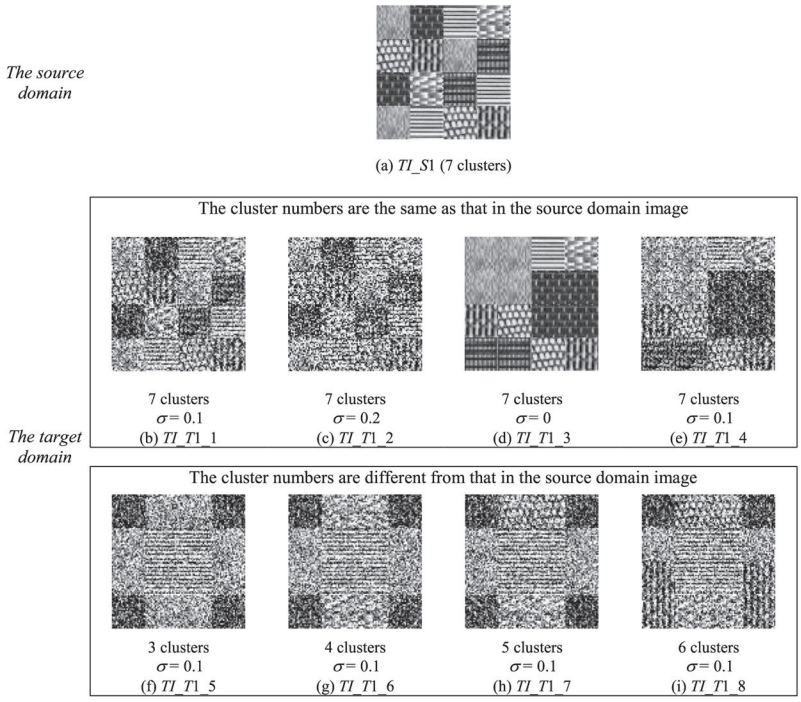

Fig. 4.

Artificial scenario 1 for transfer clustering. (a) *TI_S* 1: the image acting as the source domain; (b)–(e) *TI_T* 1_1 to *TI_T* 1_4: the target domain images owning the same cluster number as that in *TI_S* 1, but different data distributions; (f)–(i) *TI_T* 1_5 to *TI_T* 1_8: the target domain images whose cluster numbers are different from that of *TI_S* 1.

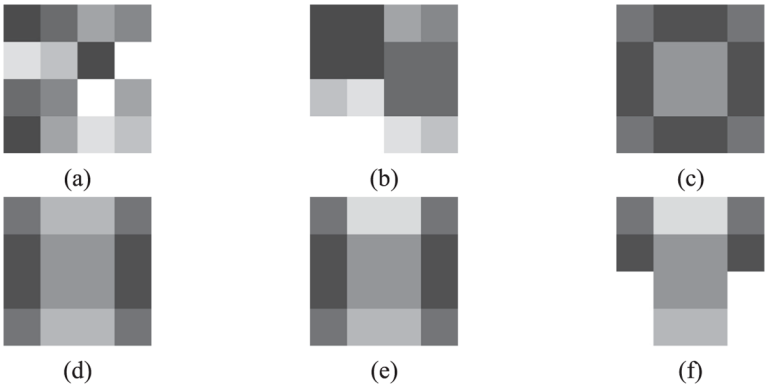

Fig. 5.

Illustrations of ideal segmentation of employed texture images. (a) for *TI_T*1_1 and *TI_T*1_2; (b) for *TI_T*1_3 and *TI_T*1_4; (c) for *TI_T*1_5; (d) for *TI_T*1_6; (e) for *TI_T*1_7; (f) for *TI_T*1_8.

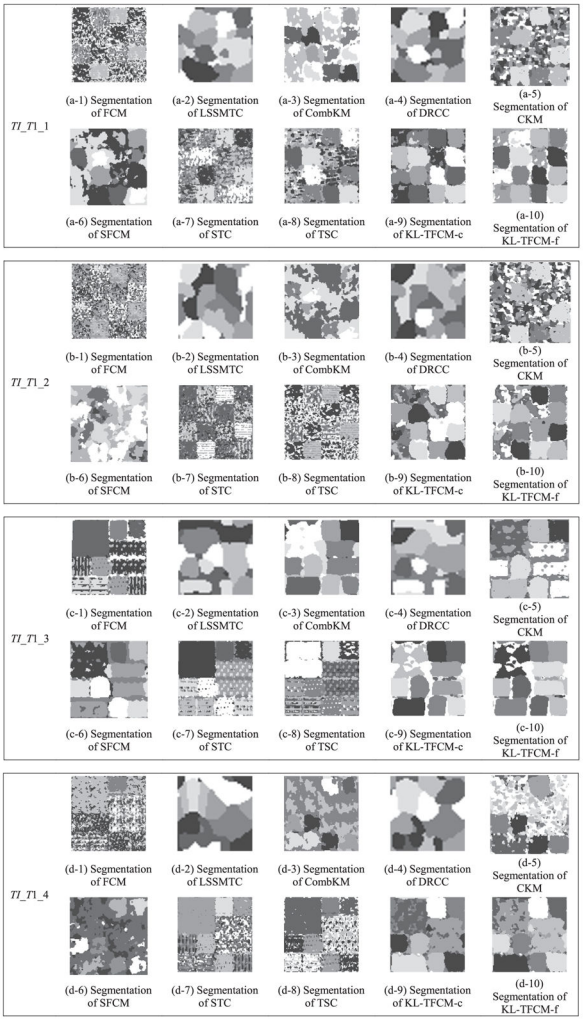

Fig. 6.

Segmentation results of ten clustering approaches on target texture images *TI_T*1_1 to *TI_T*1_4.

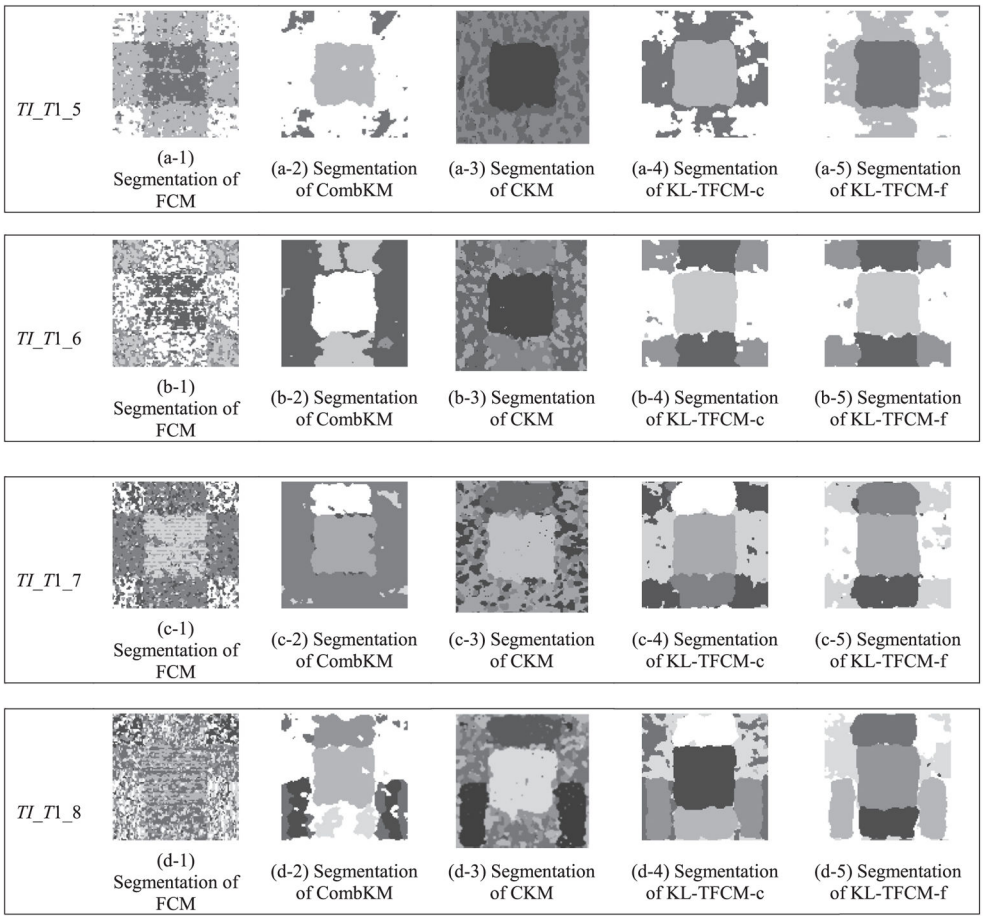

Fig. 7.

Segmentation results of five clustering approaches on target texture images *TI_T*1_5 to *TI_T*1_8.

Table 1

Common notations used throughout this manuscript.

Symbol	Use	Meaning
$X = \{\mathbf{x}_1,...\mathbf{x}_N\} \in R^{N\times D}$	Eq. (1)	The target data set with N data instances and D dimensions
$X_T = \{\mathbf{x}_{1,T},...\mathbf{x}_{N_T,T}\} \in R^{N_T \times D}$	Eqs. (5) and (12)	The data set in the target domain with N_T data instances and D dimensions
$\mathbf{U} = [\mu_{ij}]_{C\times N}$	Eq. (1)	The $C\times N$ membership matrix with μ_{ij} indicating the membership degree of $\mathbf{x}_j(j = 1,..., N)$ belonging to cluster $i(i = 1,\ldots, C)$
$\mathbf{U}_T = [\mu_{ij,T}]_{C_T\times N_T}$	Eqs. (5) and (12)	The generated $C_T \times N_T$ membership matrix in the target domain with $\mu_{ij,T}$ indicating the membership degree of $\mathbf{x}_j(j = 1,..., N_T)$ belonging to cluster $i(i = 1,\ldots, C_T)$
$\mathbf{P}_{T\&S} = [p_{jk}]_{C_T\times C_S}$	Eq. (5)	The matching degree matrix with p_{jk} indicating the matching degree of the jth estimated cluster prototype in the target domain to the kth cluster prototype in the source domain; C_T and C_S denote the cluster numbers in the target and source domains respectively
$\mathbf{V} = [\mathbf{v}_1,\cdots,\mathbf{v}_C]^T$	Eq. (1)	The cluster prototype matrix with $\mathbf{v}_i = [v_{i1}, \cdots, v_{iD}]^T$ $(i = 1,..., C)$ signifying the ith cluster prototype (centroid)
$\mathbf{V}_T = [\mathbf{v}_{1,T}, \cdots, \mathbf{v}_{C_T,T}]^T$	Eqs. (4),(5),(11), and (12)	The cluster prototype matrix in the target domain with $\mathbf{v}_{j,T} = [v_{j1,T}, \cdots, v_{jD,T}]^T$ $(j = 1,..., C_T)$ signifying the jth cluster prototype (centroid)
$\mathbf{V}_T^r = [\mathbf{v}_{1,T}^r, \cdots, \mathbf{v}_{C_T,T}^r]^T$	Generated in the knowledge matching stage, and used in the knowledge utilization stage	The raw cluster prototypes in the target domain estimated by KL-PM with $\mathbf{V}_{j,T}^r = [v_{j1,T}^r, \cdots, v_{jD,T}^r]^T$ $(j = 1, \ldots, C_T)$ signifying the jth raw cluster prototype (centroid)
$\mathbf{V}_S = [\mathbf{v}_{1,S}, \cdots, \mathbf{v}_{C_S,S}]^T$	Eqs. (4),(5), and (11)	The cluster prototype matrix in the source domain with $\mathbf{v}_{k,S} = [v_{k1,S}, \cdots, v_{kD,S}]^T$ $(k = 1,..., C_S)$ signifying the kth cluster prototype (centroid)
$\tilde{\mathbf{V}}_S = [\tilde{\mathbf{v}}_{1,S}, \cdots, \tilde{\mathbf{v}}_{C_T,S}]^T$	Eqs. (9)–(12); Generated in the knowledge matching stage, and used in the knowledge utilization stage	The employed cluster representatives from the source domain for the eventual knowledge utilization in the target domain with $\tilde{\mathbf{v}}_{j,S} = [\tilde{v}_{j1,S}, \cdots, \tilde{v}_{jD,S}]^T$ $(j = 1,..., C_T)$ denoting the jth cluster representative in the source domain

Table 2

Parameter settings in transfer clustering algorithms.

Settings	Transfer clustering algorithms		
	KL-TFCM-c/-f	**TSC**	**STC**
Core parameters	The fuzzifers m, m_1, $m_2 = \frac{\min(N, D-1)}{\min(N, D-1)-2}$, where N and D are the data size and data dimension in the target dataset, respectively; Parameters $\beta_4 \in \{0.1, 0.5, 1, 5, 10, 50, 100, 500, 1000\}$ and $\lambda^* \in \{0, 0.005, 0.1, 0.5, 0.7, 1, 1.5, 5, 10, 50, 100\}$; $\tilde{\mathbf{v}}_{j,S} \in \tilde{\mathbf{V}}_S$, $j \in [1, C_T]$, Case-c: Eq. (9) and Case-f: Eq. (10)	Parameters $K = 27$, $\lambda = 3$, and $step = 1$. For the details regarding parameters in TSC and STC, please refer to [31,32].	Trade-off parameter $\lambda = 1$

Note:

* denotes that the optimal settings need to be eventually determined by the grid search.

Table 3

Parameter settings in other algorithms.

Settings	Other algorithms					
	Classic fuzzy clustering	Multi-task clustering		Co-clustering	Semi-supervised clustering	Supervised clustering
	FCM	LSSMTC	CombKM	DRCC	CKM	SFCM
Core parameters	The fuzzifier $m = \frac{\min(N, D-1)}{\min(N, D-1) - 2}$, where N and D are the data size and data dimension, respectively; C equals the number of clusters.	Task number $T = 2$; Regularizer $l^* \in \{2, 2^2, 2^3, 2^4\}$ U[100: 100: 1000]; Regularizer $\lambda^* \in \{0.25, 0, 5, 0.75\}$	K equals the number of clusters	Regularizer $\lambda^* = \mu^* \in \{0.1,1,10, 100,500,1000\}$ See [51] for the detailed parameters	K equals the number of clusters	The fuzzifier $m = \frac{\min(N, D-1)}{\min(N, D-1) - 2}$, where N and D are the data size and data dimension, respectively;

Note:

* denotes that the optimal settings need to be eventually determined by the grid search.

Table 4

Performance comparisons of ten involved algorithms on *TI_T*1_1 to *TI_T*1_8.

Data sets	Validity Metrics	FCM	LSSMTC	CombKM	DRCC	CKM	SFCM	STC	TSC	KL-TFCM-c	KL-TFCM-f
*TI_T*1_1	NMI-mean	0.4151	0.2508	0.2500	0.2480	0.3762	0.4468	0.4986	0.5133	0.6287	**0.6336**
	NMI-std	0.0052	0.0191	0.0308	0.0213	0.0068	0.0295	0	0.0066	0.0084	0.0049
	RI-mean	0.8268	0.7893	0.7532	0.7905	0.8342	0.7882	0.8690	0.8772	0.9055	**0.9063**
	RI-std	0.0087	0.0043	0.0154	0.0037	0.0021	0.0126	0	0.0022	0.0020	0.0011
*TI_T*1_2	NMI-mean	0.3027	0.2331	0.2311	0.2264	0.2999	0.2836	0.3696	0.3470	**0.5362**	0.5350
	NMI-std	0.0048	0.0237	0.0481	0.0188	0.0169	0.0444	0	0	0.0140	0.0091
	RI-mean	0.7777	0.7695	0.7063	0.7783	0.8156	0.6630	0.7839	0.7708	**0.8600**	0.8569
	RI-std	0.0052	0.0050	0.0287	0.0015	0.0021	0.0764	0	0	0.0170	0.0124
*TI_T*1_3	NMI-mean	0.6039	0.6087	0.6092	0.3422	0.5738	0.5713	**0.6511**	0.6104	0.6200	0.6198
	NMI-std	0.0359	0.0326	0.0240	0.0241	0.0513	0.0312	0	5.77e–004	0.0037	0.0032
	RI-mean	0.8553	0.8710	0.8611	0.7849	0.8463	0.8534	**0.8877**	0.8726	0.8643	0.8644
	RI-std	0.0185	0.0112	0.0268	0.0204	0.0270	0.0195	0	2.31e–004	0.0010	0.0008
*TI_T*1_4	NMI-mean	0.4557	0.4789	0.4261	0.2413	0.4109	0.2836	0.5497	0.5511	0.6136	**0.6147**
	NMI-std	0.0197	0.0013	0.0193	0.0143	0.0015	0.0240	0	0	0.0006	0.0011
	RI-mean	0.8178	0.8185	0.8082	0.7848	0.7956	0.6598	0.8472	0.8496	0.8754	**0.8757**
	RI-std	0.0044	0.0028	0.0073	0.0013	2.96e–04	0.0363	0	0	0.0005	0.0008
*TI_T*1_5	NMI-mean	0.4644	–	0.5557	–	0.4103	–	–	–	0.6006	**0.6501**
	NMI-std	0.0002	–	0.0201	–	0.0021	–	–	–	0	7.06e–05
	RI-mean	0.7817	–	0.7310	–	0.6895	–	–	–	0.8021	**0.8360**
	RI-std	0.0001	–	0.0220	–	0.0012	–	–	–	0	5.90e–05
*TI_T*1_6	NMI-mean	0.2680	–	0.5087	–	0.5082	–	–	–	0.7398	**0.7628**
	NMI-std	0.0050	–	0.0690	–	0.0055	–	–	–	1.35e-16	1.11e–16
	RI-mean	0.6872	–	0.6578	–	0.7943	–	–	–	0.9103	**0.9168**
	RI-std	0.0020	–	0.0888	–	0.0028	–	–	–	1.35e-16	1.35e–16
*TI_T*1_7	NMI-mean	0.2910	–	0.5769	–	0.4239	–	–	–	0.7227	**0.7278**
	NMI-std	0.0080	–	0.0189	–	0.0014	–	–	–	7.85e-17	0
	RI-mean	0.7325	–	0.7347	–	0.7911	–	–	–	0.9085	**0.9054**
	RI-std	0.0033	–	0.0476	–	7.03e–04	–	–	–	0	0

Data sets	Validity Metrics	FCM	LSSMTC	CombKM	DRCC	CKM	SFCM	STC	TSC	KL-TFCM-c	KL-TFCM-f
TI_TI_8	NMI-mean	0.2038	–	0.5728	–	0.5190	–	–	–	0.6827	**0.6914**
	NMI-std	0.0225	–	0.0329	–	0.0019	–	–	–	0.0005	1.11e–16
	RI-mean	0.7399	–	0.7941	–	0.8615	–	–	–	0.9010	**0.9032**
	RI-std	0.0059	–	0.0160	–	6.58e–04	–	–	–	0.0002	0